Anatomical and functional MR imaging to define tumoral boundaries and characterize lesions in neuro-oncology

Joseph Benzakoun, Charlotte Robert, Laurence Legrand, Johan Pallud, Jean-François Méder, Catherine Oppenheim, Frédéric Dhermain, Myriam Edjlali

Cancer / Radiotherapie

Anatomical and functional MR imaging to define tumoral boundaries and characterize lesions in neuro-oncology

--Manuscript Draft--

Manuscript Number:	CANRAD-D-19-00218
Article Type:	Revue generale/General review
Section/Category:	Submission for a Special Issue / Article pour un numéro thématique
Keywords:	Brain tumors; Neuroimaging; Perfusion MRI; Proton magnetic resonance spectroscopy; tumor segmentation; Radiomics; dose painting
Corresponding Author:	Joseph Benzakoun FRANCE
First Author:	Joseph Benzakoun
Order of Authors:	Joseph Benzakoun
	Charlotte Robert
	Laurence Legrand
	Johan Pallud
	Jean-François Meder
	Catherine Oppenheim
	Frederic Dhermain
	Myriam Edjlali
Abstract:	Neuroimaging and especially MRI has emerged as a necessary imaging modality to detect, measure, characterize and monitor brain tumors. Advanced MRI sequences such as perfusion MRI, diffusion MRI and spectroscopy as well as new post-processing techniques such as automatic segmentation of tumors and radiomics play a crucial role in characterization and follow up of brain tumors. The purpose of this review is to provide an overview on anatomical and functional MR imaging use for brain tumors boundaries determination and tumor characterization in the specific context of radiotherapy. The usefulness of anatomical and functional MR imaging on particular challenges posed by radiotherapy such as pseudoprogression and pseudoresponse and new treatment strategies such as dose painting is also described.

Jean-Jacques Mazeron
Rédacteur en Chef
Cancer / Radiothérapie

Cher Pr Mazeron,

Merci de trouver en pièce jointe le manuscrit intitulé "*Imagerie fonctionnelle pour la définition des volumes cibles et la caractérisation des lésions en neuro-oncologie"*, que nous soumettons auprès de Cancer / Radiothérapie sur votre sollicitation. Cet article est conçu pour s'intégrer dans le numéro Spécial Imagerie, coordonné par Philippe Giraud, Pierre Véra et Laure Fournier. Il est rédigé en anglais et apporte un point de vue sur l'imagerie diagnostique et fonctionnelle, pré et post-thérapeutique des tumeurs cérébrales primitives et secondaires.

Nous souhaiterions que les deux derniers auteurs (F. Dhermain et M. Edjlali) soient déclarés en tant que co-derniers auteurs si cela est possible, du fait de leur contribution équivalente dans la rédaction de cet article.

Nous restons à votre disposition pour toute information complémentaire,

Cordialement,

Myriam Edjlali, MD, PhD Joseph Benzakoun, MD, MSc

Anatomical and functional MR imaging to define tumoral boundaries and characterize lesions in neuro-oncology

Imagerie fonctionnelle pour la définition des volumes cibles et la caractérisation des lésions en neuro-oncologie

Joseph BENZAKOUN [a*,b,c,d], Charlotte ROBERT [e,f,g,h], Laurence LEGRAND [a,b,c,d], Johan PALLUD [b,c,d,i], Jean-François MÉDER [a,b,c,d], Catherine OPPENHEIM [a,b,c,d], Frédéric DHERMAIN [j,1], Myriam EDJLALI [a,b,c,d,1]

[a] Radiology Department, GHU Paris, centre hospitalier Sainte-Anne, 1 rue Cabanis, 75014 Paris, France

[b] Université de Paris, 85, boulevard Saint-Germain, 75006 Paris, France

[c] Imabrain, Institut de psychiatrie et neurosciences de Paris (IPNP), 102–108 rue de la Santé, 75014 Paris, France

[d] Inserm, U1266, 102 rue de la Santé, 75013 Paris, France

[e] Medical Physics Department, Gustave-Roussy, 114, rue Édouard-Vaillant, 94805 Villejuif, France

[f] Molecular Radiotherapy, Gustave-Roussy, 114, rue Édouard-Vaillant, 94805 Villejuif, France

[g] Inserm, 114, rue Édouard-Vaillant, 94805 Villejuif, France

[h] Paris-Sud University, Paris-Saclay University, 114, rue Édouard-Vaillant, 94805 Villejuif, France

[i] Neurosurgery Department, GHU Paris, centre hospitalier Sainte-Anne, 1 rue Cabanis, 75014 Paris, France

[j] Radiotherapy Department, Gustave-Roussy, 114, rue Édouard-Vaillant, 94805 Villejuif, France

***Corresponding author**: Joseph Benzakoun; tel. +33 1 45 65 72 00; E-mail : j.benzakoun@ghu-paris.fr

[1] These authors contributed equally as last authors.

Abstract

Neuroimaging and especially MRI has emerged as a necessary imaging modality to detect, measure, characterize and monitor brain tumours. Advanced MRI sequences such as perfusion MRI, diffusion MRI and spectroscopy as well as new post-processing techniques such as automatic segmentation of tumours and radiomics play a crucial role in characterization and follow up of brain tumours. The purpose of this review is to provide an overview on anatomical and functional MRI use for brain tumours boundaries determination and tumour characterization in the specific context of radiotherapy. The usefulness of anatomical and functional MRI on particular challenges posed by radiotherapy such as pseudo progression and pseudo esponse and new treatment strategies such as dose painting is also described.

Keywords

Brain tumours, Neuroimaging, Perfusion MRI, Proton magnetic resonance spectroscopy, tumour segmentation, radiomics, dose painting

Résumé

Les avancées en neuro-imagerie, principalement liées au développement de l'IRM, ont rendu cette modalité centrale dans la prise en charge des patients porteurs de tumeur cérébrale. L'IRM, par son approche anatomique, permet de détecter, localiser et caractériser les lésions. L'application de séquences avancées d'IRM de type imagerie de perfusion, de spectroscopie ou de diffusion, ainsi que les nouveaux post-traitements permettant une segmentation ou une caractérisation automatique des lésions, apportent de nouvelles possibilités pour affiner la caractérisation des tumeurs tant au moment du diagnostic initial que lors du traitement par radiothérapie et du suivi. Le but de cette revue de littérature est de donner un aperçu de l'utilisation des imageries IRM anatomique et fonctionnelle utilisées pour la détermination des contours des différentes tumeurs cérébrales dans le contexte particulier de la radiothérapie. L'utilité de l'IRM anatomique et fonctionnelle est également examinée, en portant une attention particulière aux défis posés par la radiothérapie, tels que la pseudoprogression et la pseudoréponse, ainsi que par de nouvelles stratégies de traitement personnalisées, comme la *dose painting*.

Mots-clés

Tumeurs cérébrales, neuroimagerie, IRM de perfusion, spectroscopie magnétique, segmentation tumorale, radiomique, *dose painting*

1. Introduction

Brain tumour detection and characterization rely on standard imaging with computed tomography (CT) and magnetic resonance (MR) routinely used for this purpose. Thanks to its superior soft tissue contrast to delineate tumours, MR has emerged as a necessary imaging modality. Beyond its anatomical advantage, advanced multimodal MRI techniques, as well as PET MRI and new post processing techniques, including artificial intelligence applied to image analysis, open new possibilities of characterizing tumours. Hence, neuroimaging has evolved into a comprehensive diagnostic tool at each step of the patient care: detection and characterization of morphological properties of the tumour, evaluation of malignant transformation of low-grade gliomas, choice of treatment strategies, monitoring of treatment response and prognosis definition. The purpose of this review is to provide an overview of morphologic and functional MRI used to assess brain tumours boundaries and the different challenges for radiotherapy purposes.

2. Detection and delineation of intraparenchymal brain tumours

2.1. MR acquisition protocol

The conventional structural radiotherapy MR protocol is constructed based on several requirements: detection, characterization and anatomical delineation. Each of these requirements are completed by one or more specific MR acquisition sequences that we will be described. Attempts for standardization of these sequences and their parameters for clinical trials have been made in 2015 by US neuro-oncology experts, in order to unify protocols for multicentre studies [1]. Each sequence of the MR acquisition protocol must be thoroughly optimized in order to improve the contrast-to-noise ratio and to reduce scan time, with a total acquisition time of 30 minutes or less to be compatible with clinical routine. The proposed protocol contains: T1- and T2-weighted sequences, T2-weighted sequence with fluid-attenuated inversion recovery (FLAIR), diffusion-weighted imaging (DWI), and T1-weighted sequence after contrast enhancement (Fig. 1).

2.1.1. T1-weighted sequences and T1-weighted sequences after contrast enhancement

T1-weighted sequence and T1-weighted sequence after contrast enhancement reflect the enhancing part of a tumour, which is present in a vast majority of primary and secondary brain tumours given the nonspecific breakdown of the blood–brain barrier. This disruption is responsible for a leakage of gadolinium into the extracellular spaces of the tumour. The gadolinium element, used as MR contrast agent, is strongly paramagnetic at low concentrations, and is responsible for a T1 shortening effect

which increases the T1 signal within the tumour, providing strong contrast compared to normal tissues. This strong contrast allows the detection of small (less than 5mm) lesions, especially brain metastases [2,3] . Several parameters can improve the detection rate of small lesions.

2.1.1.1. Contrast agent dose

The detection rate increases with the dose of contrast agent [4]. However, increasing the dose is not recommended in clinical practice even with modern contrast agents due to unknown effects of in-vivo gadolinium long-term deposition in patients with repeated contrast injection [5,6] .

2.1.1.2. Magnetic field

Using a high field intensity MR increases the contrast-to-noise ratio and allows to reduce the contrast agent dose at 3 T as compared to 1.5 T [7]. Recent studies assessing very high field scanners have confirmed this effect at 7 T [8].

2.1.1.3. Time delay between injection and acquisition

As blood–brain barrier disruption is time-dependent, the degree of enhancement has been shown to increase with time, and it is recommended to acquire the T1-weighted sequence after contrast enhancement sequence 10 to 15 minutes after contrast agent injection [9].

2.1.1.4. Sequence type

Two main sequence types can be used for performing T1-weighted imaging: gradient echo imaging (T1w-GRE), which has been used for 25 years for its speed and three-dimensional (3D) capabilities [10]. More recently, studies have found a higher rate of metastasis detection with thin-slice spin echo imaging (T1w-SE) [11]. The consensus is currently unclear on which sequence type should be used in clinical routine, but a shift towards T1-weighted spin echo is highly likely in years to come.

2.1.1.5. Use of subtraction techniques

Acquiring T1-weighted sequences with and without injection of contrast agent allows to compute a subtraction map, which has a great value for evaluating haemorrhagic lesions that can have a spontaneous high T1 signal and to improve contrast and lesion delineation (Fig. 2) [12,13].

Regarding characterization, the T1-weighted sequence after contrast enhancement gives several morphological elements for orienting tumour type [14]. These include localization of the tumour (intra- vs. extra-axial) and its core characteristics (necrotic, cystic or solid).

When evaluating tumour after radiation therapy, T1-weighted sequence after contrast enhancement yields some morphologic factors that can help to distinguish radiation necrosis from recurrence. Typically, corpus callosum involvement, apparition of multiple enhancement foci and subependymal spread are suggestive of tumoral recurrence but these features are often insufficient alone to be conclusive [15].

At last, T1-weighted sequence and especially T1-weighted gradient echo sequence, with its high resolution and high gray–white matter contrast, helps the anatomical localization of radiosensitive brain structures such as optic nerve, cochlea, hippocampus, brainstem, pituitary gland, circle of Willis [16].

2.1.2. FLAIR sequence

The FLAIR sequence is a T2-weighted sequence with an additional inversion recovery pulse that allows a suppression of the cerebrospinal fluid signal and is therefore sensitive to infiltrative oedema.

In untreated brain metastasis, a high intensity area surrounding an enhanced tumour is linked to vasogenic oedema. This reactional oedema does not contain tumoral cells and as such is not considered as a target for radiotherapy. In diffuse gliomas, the non-enhancing high intensity areas in FLAIR have a different origin. They correspond to a mixture of vasogenic oedema and tumour infiltration (Fig. 3). Low-grade gliomas are mostly described as diffuse infiltrating tumours with high FLAIR signal and no contrast enhancement on T1-weighted sequence. In high-grade gliomas, infiltrative high intensity FLAIR regions are observed in periphery of an enhanced nodule [17]. In both cases, infiltration displays different characteristics as compared to vasogenic oedema including cortex and basal ganglia involvement, corpus callosum extension, or focal mass effect. In radiation therapy, there is still no full consensus regarding whether the FLAIR hyperintensities should be included in gross tumour volumes [18,19]. Recent studies have proposed morphological and functional methods to differentiate glial infiltration from oedema within the high intensity zone but are not yet used in clinical practice [20,21].

After antiangiogenic therapy of a glioblastoma, a regression of the enhanced portion can falsely be interpreted as a response to treatment but may be due to a normalization of the blood–brain barrier rupture without real tumour decrease. In this particular setup, a fine analysis of the FLAIR sequence is essential for tumour response evaluation [22].

2.1.3. T2-weighted sequence

T2-weighted sequence given information is close to FLAIR sequence and does not bring much additional information on a given tumour. As liquid tissues yield high T2 signal, T2 sequence can possibly help the characterization of cystic or necrotic portions in a tumour. Moreover, T2 may have a value for automatic segmentation because of its high anatomical contrast (see paragraph 2.3).

2.1.4. Diffusion-weighted imaging sequence

The diffusion-weighted imaging sequence is at the junction of morphological and functional imaging. In the context of brain tumour exploration, a diffusion coefficient restriction is evidence for high cellularity [23]. Diffusion has shown its relevance for grading non-enhancing glioma and for the

diagnosis of lymphoma [24,25]. Moreover, it is essential in early postoperative context, where it allows to diagnose ischemic injury whose imaging evolution can be confused with tumour recurrence and help the detection of potential infectious complications such as abscesses [26].

2.1.5. Other morphological sequences

T2* or T2 gradient echo and susceptibility-weighted imaging are widely used at the diagnosis stage in order to evaluate brain tumour haemorrhage content. Among primitive cerebral tumours, glioblastoma, astrocytoma and oligodendroglioma are prone to be haemorrhagic [27]. For secondary tumours, haemorrhage is classically observed in melanoma, choriocarcinoma, renal cell carcinoma, thyroid cancer, but also in lung and breast cancer due to their high prevalence [28].

2.2. Bidimensional versus three-dimensional volumes

In the early days of MRI, spin echo bidimensional (2D) sequences were the most popular sequences because of their acquisition time (compatible with clinical practice) and their robustness to magnetic field inhomogeneity [29]. In the early 1990s, 3D T1-weighted and T2-weighted sequence acquisitions became available due to the technological progresses [30]. In addition, the rapid development of computer post-treatment allowed to reformat dynamically 3D sequences in axial, sagittal, coronal and oblique planes. These elements are now essential for lesion characterization and treatment planning, and nowadays all T1-weighted sequence after contrast enhancement are acquired in 3D.

Three-dimensional FLAIR sequences are now also considered clinical routine. They are especially relevant for the study of glioma where the tumoral infiltration is not homogeneous in space. Even if 2D FLAIR is currently the basis for initial diagnosis recommendations, this may change in the years to come [31].

Three-dimensional sequences are of special interest when planning conformal radiation therapy, as registration of 3D sequences onto CT is easier than with 2D images, and the quality of this registration can affect the target delineation and the resulting treatment plan [32].

2.3. RANO measurement criteria

Identifying more effective brain tumour therapies was several years ago partially limited by the lack of reliable criteria to determine tumour response and progression. In neuro-oncology, this evaluation was especially difficult since contrast enhancement operates as an incomplete surrogate for tumour assessment and is affected by agents that influence vascular permeability, such as antiangiogenic therapy. Moreover, most tumours have a non-enhancing component which may be difficult to quantify.

Although the RECIST criteria are widely used to assess the response to systemic cancer therapies, their use in neuro-oncology have been limited by the fact that 1D measurements may not accurately

reflect irregular and asymmetric shapes. The Response Assessment in Neuro-Oncology (RANO) working group was established to improve the characterization of tumour evolution, assessment of tumour response and selection of end points, specifically in the context of clinical trials [33–35]. The RANO working group was originally created to update response criteria for high- and low-grade gliomas and to address issues such as pseudo response and non-enhancing tumour progression during antiangiogenic therapies, and pseudo progression during chemo-radiotherapies. It was then extended to other brain tumours including brain metastases, leptomeningeal metastases, spine tumours, paediatric brain tumours, and meningiomas.

2.3.1. Glioblastomas

In reaction to the need for better standardization of image acquisition for glioblastoma, a recent consensus paper was published detailing an "international brain tumour imaging protocol (BTIP)" with recommended sequences and parameters [36,37]. Parameter matched, pre- and post-contrast 3D inversion recovery gradient recalled echo (IR-GRE) images with less than 1.5 mm isotropic resolution, are at the heart of this suggested method, allowing for bidimensional and volumetric measurements of the enhancing part of the tumour. Based on the RANO criteria, tumour response should be determined in comparison to the tumour measurements obtained at pretreatment baseline, and tumour progression should be concluded based on the comparison of post-treatment images to the smallest tumour measurement at either pretreatment baseline or after initiation of therapy.

Quantification of contrast enhancing tumour size or volume should be performed on contrast-enhanced T_1-weighted digital subtraction maps in order to improve the lesion visualization.

Two-dimensional, perpendicular measurements of contrast enhancing tumour size, excluding the resection cavity along with any cysts or areas of central macroscopic necrosis, should be used for response assessment if volumetric tools are not available (Fig. 4).

Measurable disease should be defined as contrast enhancing lesions with a minimum size of both perpendicular measurements greater than or equal to 10 mm. Up to five target measurable lesions should be described and ordered from the largest to the smallest. Non-measurable disease should be defined as lesions that are too small (less than 1 cm in both perpendicular dimensions), non-enhancing, or lesions that contain a poorly defined margin that cannot be measured or segmented with confidence.

To avoid interpretation of postoperative changes as residual enhancing disease, a baseline MRI scan should ideally be obtained within 24 to 48 hours after surgery and no later than 72 hours [38].

Because novel treatments are likely to result in a higher than normal incidence of treatment-related increase in contrast enhancement ("pseudo progression") or decrease in contrast enhancement ("pseudo response"), patients should continue therapy with close observation (e.g. 4 to 8 week

intervals) if there is a suspicion of pseudo progression or pseudo response (see paragraph 3.2.4). If subsequent imaging studies and/or clinical observations demonstrate that progression has actually occurred, the date of confirmed progression should be noted as the scan at which the potential progression was first identified. This is especially true for immunotherapy response, for which specific iRANO modified criteria have been developed to address the challenges of emerging novel immunotherapy for high-grade gliomas [39]. Indeed, a form of pseudoprogression is encountered in immunotherapy that is distinct from that seen in routine chemoradiotherapy (Stupp protocol) both in mechanism and imaging appearances.

2.3.2. Lower grade gliomas

The RANO criteria for low-grade gliomas cannot rely on enhancing lesions, as most of the time these are unenhanced lesions. The classification is therefore based on percentage of T2/FLAIR signal modification [40]. In addition, since modifications are usually evolving mildly, the RANO low-grade glioma criteria introduce minor response category (greater than 25% but less than 50% decrease in area). As with RANO- high-grade gliomas, corticosteroid use and clinical status are considered in the determination of response and progression.

One of the challenges in determining response and progression in low-grade gliomas is the difficulty in accurately measuring the tumour using only 2D tools. It is important to refer to baseline scanner each comparison and ongoing work should determine if measuring T2/FLAIR volume is more accurate than 2D measurements to distinguish changes in tumour size. Volume growth trajectory could also be a more adapted measure of response. [41]

2.3.3. Brain metastasis

The RANO-brain metastasis (RANO-BM) working group developed normative criteria for determining response criteria in brain metastasis studies based upon factors derived from RANO-high-grade gliomas and RECIST [42,43]. In these criteria, 1D measurement is used to assess the larger diameter. As with RECIST, the sum of the diameters for all target lesions are to be calculated and the sum of longest diameters has to be reported at baseline. All other central nervous system lesions such as leptomeningitis, small lesions less than 1cm, or cystic only lesions should be identified as non-target lesions and should also be recorded at baseline.

Progression occurs when the sum of the linear measurements exceeds 20% compared with baseline or best response. In addition to the relative increase of 20%, at least one lesion must increase by an absolute value of 5 mm or more to be considered progression.

For non-target lesions, unequivocal progression of existing enhancing non-target central nervous system lesions, new lesion(s) (except while on immunotherapy-based treatment), or unequivocal progression of existing tumour-related non-enhancing (T2/FLAIR) central nervous system lesions define progression.

Partial response is defined as reduction of the sum of linear measurements by 30% compared with baseline, sustained for at least 4 weeks without any new lesion, under stable to decreased clinical symptoms and corticosteroid dose.

3. Advanced magnetic resonance imaging of intraparenchymal brain tumours

Analysing morphological MRI often allows the clinician to give an accurate picture of the nature or the evolution of a tumour, but in a certain proportion of cases, advanced methods allow to increase confidence in differential diagnosis, pretherapeutic planning, tumour grading and follow-up findings [44]. The European Society of Neuroradiology (ESNR) Annual Meeting 2015 workshop recommended an imaging protocol for glioma diagnosis and emphasized on the role of advanced MRI modalities in routine [45].

After a quick review of the technical aspects of each advanced sequence available in clinical practice, examples of clinical applications will be described.

3.1. Advanced sequences

3.1.1. Diffusion weighted imaging and diffusion tensor imaging

Diffusion-weighted imaging is correlated to the Brownian motion of water molecules in tissue in the three dimensions. The apparent diffusion coefficient (ADC), which reflects the water molecules diffusion, decreases as the cellularity in a tissue increases [23]. This decrease is especially noted for several high cellularity tumour types such as lymphoma [25]. Diffusion tensor imaging is based on the same principle as diffusion-weighted imaging, but with a higher number of explored dimensions, is able to evaluate the preferential direction of white matter fibres within a voxel. This is often summarized with a scalar number, fractional anisotropy (FA), which characterizes the directionality of fibre within each voxel. Diffusion tensor imaging also allows the visualization of main white matter fascicles and can be integrated into radiotherapy planning in order to reduce white matter damage [46] .

3.1.2. Perfusion MRI

Two types of perfusion imaging have been proposed in the literature:

- dynamic susceptibility imaging, which has a high temporal resolution, and allows to explore the neoangiogenesis of a tumour. The arterialization of a tumour if often characterized by the relative cerebral blood volume, which is increased in case of neoangiogenesis [47];
- dynamic contrast enhancement imaging, which has lower temporal resolution but better spatial resolution, allows to evaluate the capillary permeability of a lesion synthesized into the Ktrans scalar value [48].

3.1.3. MR spectroscopy

MR spectroscopy aims at performing in vivo chemical spectroscopy, in order to evaluate the relative quantity of different metabolites in brain parenchyma [49]. Most frequent metabolites are creatine, myoinositol mainly concentrated within glial cells, choline, which is related to cell membrane turnover, *N*-acetyl-aspartate, which is mainly concentrated within the neurons, lactates, which are related to hypoxia and lipids, which are related to necrosis. Some metabolites may even be suggestive for certain tumoral types, such as alanine for meningioma or taurine for medulloblastoma [50,51].

Classic spectroscopy is made in a single voxel but some multi-voxel techniques allow to acquire spectra over a 2D or 3D volume, allowing a sampling of the different parts of a tumour [49].

3.2. Application of advanced sequences in clinical situations

3.2.1. Differential diagnosis

Pseudo tumours such as pseudo tumoral multiple sclerosis can be misleading when unique and enhancing. Several morphological criteria can help to evoke this diagnosis as a white matter involvement, a ring pattern or an open ring enhancement [52]. Advanced techniques increase the diagnostic confidence by adding quantitative features such as a peripheral ADC restriction and a choline/*N*-acetyl-aspartate ratio ≤ 1 on MR spectroscopy (Figure S1) [53,54]. However, these findings are inconstant and must be interpreted with caution and only in conjunction with morphologic imaging.

3.2.2. Tumour type characterization

Advanced sequences may help the diagnosis of certain tumour types. For example, primary cerebral nervous system lymphomas have a classical presentation on both diffusion-weighted imaging and dynamic susceptibility contrast perfusion that may help the differential diagnosis with glioma [55,56]. For these tumours, a high diffusion signal with an ADC restriction is observed. In perfusion sequence, primary cerebral nervous system lymphoma is not associated with elevated relative cerebral blood volume but can show a classical blood–brain barrier rupture characteristic with a signal intensity curve returning above the baseline (Figure S2) [57]. At last, on MR spectroscopy, primary cerebral nervous system lymphoma can demonstrate high choline/creatine ratios and elevated lipids.

Differentiation of glioblastoma and metastasis is frequently an issue when the morphology is not specific, especially when the enhanced lesion is unique, and the peritumoral FLAIR hyperintensities do not obviously infiltrate the gray matter or the corpus callosum. In such situations, multimodal imaging may be of help to differentiate them. However, as metastases can be arterialized and do not contain normal brain parenchyma, the core of a metastasis is virtually not distinguishable from the enhancing portion of a glioblastoma, as both can have hyperperfusion and tumoral spectrum on MR spectroscopy [58]. The solution is to evaluate these parameters in the surrounding FLAIR hyperintensities: in metastasis, this hyperintensity is pure oedema and does not contain tumoral cells, whereas in glioblastoma the hyperintensity can be itself tumoral. As a result, in the peritumoral oedema of a metastasis the relative cerebral blood volume will be decreased (<1), the ADC will be increased and the MR spectroscopy spectrum will be normal with a low choline/*N*-acetyl-aspartate ratio [58]. In contrast, in the non-enhancing portion of a glioblastoma, the relative cerebral blood volume may be increased (greater than 1), ADC may be lower and the choline/*N*-acetyl-aspartate ratio may be elevated (greater than 1.11). [58,59]

3.2.3. Tumour grading

Glioma grading is important for the patient care and decision-making process. Multimodal MRI can help to improve the performances of glioma grading and grade change during follow-up. Indeed, even if tumour enhancement is a marker of malignancy in glioblastoma, it is neither fully specific nor sensitive [60]. It has been shown that up to one third of non-enhancing glioma can be high grade gliomas [61]. In the absence of enhancement, hyperperfusion on perfusion-weighted imaging is a good marker for high grade glioma, with cutoff values at 1.75 for relative cerebral blood volume between grade II and III gliomas [62]. Moreover, an increase of relative cerebral blood volume in a low-grade glioma is predictive for a transformation to a higher grade glioma [63].

MR spectroscopy has also an interest in glioma grading, as transformation is characterized by increased choline/*N*-acetyl-aspartate ratio and appearance of lipid and lactates [64]. At last, susceptibility-weighted imaging, by showing the neoangiogenesis and microhaemorrhages appearing as intratumoral susceptibility signals (ITSS), has also a certain significance for tumour grading [65].

3.2.4. Tumour follow-up after treatment

3.2.4.1. Pseudo progression and radionecrosis

After radiation therapy of a tumour (metastasis or gliomas), early or tardive changes of the brain parenchyma can occur and be mistaken for tumour progression.

Pseudo progression occurs within 3 months after completing treatment and its occurrence is potentialized by *O6*-methylguanine-DNA methyltransferase status of tumour and temozolomide treatment [66]. Morphologically, it presents as fluffy enhancement around the initial tumour [67].

Diagnosis is usually made at follow-up, but elements such as an elevated ADC and a low relative cerebral blood volume on multimodal imaging can comfort this hypothesis [67].

Radiation necrosis is usually delayed 3 to 12 months after radiotherapy (up to several years after) and has a morphological aspect than can mimic a necrotic relapse of a metastasis or glioblastoma, sometimes with a classical “soap bubble” appearance [66]. In the case of radiation necrosis, ADC is elevated and relative cerebral blood volume is decreased with a cut-off between 1 and 2 varying with the studies [68]. MR spectroscopy is here limited as both treatment necrosis and tumour necrosis can contain lipids and lactates, but an increase in choline/*N*-acetyl-aspartate ratio greater than 1.8 may be a marker of recurrence rather than radiation necrosis [68,69]. At last, delayed acquisition after contrast enhancement (75min) may also help the distinction between tumour (contrast clearance) and non-tumoral tissue (contrast accumulation) [70].

Analysis may be furthermore complicated by the coexistence of radiation necrosis and recurrence. Usage of high-resolution sequences and multivoxel MR spectroscopy may be helpful in these cases [71].

3.2.4.2. Pseudo response

In case of treatment with antiangiogenic chemotherapy such as bevacizumab and cediranib, a normalization of the blood–brain barrier without tumour reduction can be observed. This can lead to a decreased enhancement of the tumour that can falsely be interpreted as tumoral response [67]. Accurate evaluation of non-enhancing tumour on FLAIR sequences and ADC maps as well as early follow-up will allow to rectify the diagnosis.

4. Advanced post processings

4.1. Automated segmentation

With the increase of 3D sequences acquired for radiation planning, the manual delineation of region of interests becomes more and more complicated. Many techniques have been proposed in order to automatically (Figure S3) or semiautomatically delineate different glioblastoma component based on multimodal imaging. Free software such as BraTumIA for automatic segmentation, or ITK-Snap and 3D Slicer are available for semi-automatic segmentation [72,73]. Recent developments tend to use deep learning as a framework for more efficient segmentations, such as the DeepMedic open-source algorithm [74].

4.2. Radiomics

Radiomics is a computer-based framework based on the extraction of hundreds of tumour features from medical images and has multiple potential applications in the context of brain lesions: improvement of diagnosis, tumour grading, treatment response monitoring, outcome and survival

prediction [75]. The “radiomics” term was proposed ten years ago [76]. The number of studies on this topic has exploded recently, with more than 90 papers focused on neuro-oncology published these last four years. Regarding diagnosis, several studies have analysed the performances of radiomics features, used alone or in association with clinical features, to differentiate glioblastoma from solitary brain metastasis using retrospective cohorts of more than 100 patients [77–80]. Based on post-contrast 3D T1-weighted image mainly, accuracy values higher than 0.78 were reported in testing sets, suggesting the ability of such machine learning tools to assist physicians in this complex task in a near future. Always in diagnosis, a large number of studies were conducted to improve tumour grading based on multiparametric MRI considering conventional sequences and more advanced techniques (diffusion, perfusion and spectroscopy MR) [81]. Results are encouraging with classifiers achieving area under the receiver operator characteristic curve superior to 0.90. More challenging studies planned to predict glioma molecular subtypes (isocitrate dehydrogenase mutation status, 6-methylguanine-DNA methyltransferase promoter methylation) using machine-learning radiomics-based models [82].

Even if radiomics sounds as an attractive domain, readers should pay attention to the reported methodology as most of MR sequences suffer from being not quantitative, with possible motion, tissue-based and magnetic fields non-homogeneity artefacts. As well, all reported results must be analysed with caution as some studies report performances results in non-independent testing sets, which can lead to hazardous non generalizable results.

4.3. Challenges in radiotherapy

As described previously, advanced MR sequences are now widely used in the clinical management of primary lesions and metastasis for diagnosis and post-treatment monitoring purposes. However, no clear consensus exists yet about the use of functional imaging to modify delineated tumour areas or implement personalized heterogeneous dose distributions also known as dose painting [83,84].

The example of dynamic susceptibility contrast perfusion demonstrates the difficulty of the choice of the relative cerebral blood volume cutoff for a delineation purpose in patients with glioblastoma, whose optimization highly depends on the criterion used in published studies [85]. The observed results variability can also be explained by the various methods existing for relative cerebral blood volume estimation [86]. Khalifa et al. have analysed the ability of dynamic susceptibility contrast MRI to predict recurrence areas in high grade gliomas treated by chemoradiotherapy and obtained negative results in a cohort of 15 patients [87]. In the same cohort, results based on diffusion-weighted imaging sequences were also inconclusive. Based on ADC maps, Orlandi et al. calculated hypofractionated dose-painting by numbers plans for five patients with recurrent glioblastoma [88]. Dosimetric results showed that only three out of five patients could receive a safe treatment. In other cases, maximal dose to organs at risk were exceeded.

More concrete results were obtained based on MR spectroscopy and metabolite ratio metrics, even if it may be still challenging to obtain reliable and reproducible spectroscopy data [89]. Laprie et al. analysed in a longitudinal study correlation of spectral and morphologic abnormalities before any radiotherapy to relapse areas for 1207 voxels [90]. They showed that 75% of the regions in which an elevated choline/*N*-acetyl-aspartate ratio (greater than 2) was observed still corresponded to an elevated choline/*N*-acetyl-aspartate ratio at relapse. These results opened the way to two clinical trials that are still active today: the French multicentre phase III SPECTRO-GLIO clinical trial (NCT01507506) evaluating the impact of a choline/*N*-acetyl-aspartate boost of 72 Gy on overall survival and the US phase II clinical trial (NCT03137888) which aim is a feasibility study and toxicity analysis. Results of these clinical trials will be of importance for the future of dose painting in treatment of glioblastoma.

Supplementary material

Supplementary figures S1-S3 available online.

Acknowledgements

The authors thank Vincent Lebon for his critical revision of the manuscript.

Author contribution

JB, FD, ME: conceptualization, investigation, writing - original draft; CR, LL, JP, JFM, CO: conceptualization, writing - review and editing.

References

1. Ellingson BM, Bendszus M, Boxerman J, Barboriak D, Erickson BJ, Smits M, et al. Consensus recommendations for a standardized brain tumor imaging protocol in clinical trials. Neuro-Oncol 2015;17(9):1188–98.

2. Pope WB. Brain metastases: neuroimaging. Handb Clin Neurol 2018;149:89–112.

3. Deike-Hofmann K, Thünemann D, Breckwoldt MO, Schwarz D, Radbruch A, Enk A, et al. Sensitivity of different MRI sequences in the early detection of melanoma brain metastases. PLoS ONE 2018;13(3):e0193946.

4. Yuh WT, Engelken JD, Muhonen MG, Mayr NA, Fisher DJ, Ehrhardt JC. Experience with high-dose gadolinium MR imaging in the evaluation of brain metastases. Am J Neuroradiol 1992;13(1):335–45.

5. Ramalho J, Semelka RC, Ramalho M, Nunes RH, AlObaidy M, Castillo M. Gadolinium-based contrast agent accumulation and toxicity: an update. Am J Neuroradiol 2016 Jul 1;37(7):1192–8.

6. Bjørnerud A, Vatnehol SAS, Larsson C, Due-Tønnessen P, Hol PK, Groote IR. Signal enhancement of the dentate nucleus at unenhanced MR imaging after very high cumulative doses of the macrocyclic gadolinium-based contrast agent gadobutrol: an observational study. Radiology 2017;285(2):434–44.

7. Krautmacher C, Willinek WA, Tschampa HJ, Born M, Träber F, Gieseke J, et al. Brain tumors: full- and half-dose contrast-enhanced MR imaging at 3.0 T compared with 1.5 T—initial experience. Radiology 2005;237(3):1014-9

8. Noebauer-Huhmann I-M, Szomolanyi P, Kronnerwetter C, Widhalm G, Weber M, Nemec S, et al. Brain tumours at 7T MRI compared to 3T—contrast effect after half and full standard contrast agent dose: initial results. Eur Radiol 2015;25(1):106–12.

9. Cohen-Inbar O, Xu Z, Dodson B, Rizvi T, Durst CR, Mukherjee S, et al. Time-delayed contrast-enhanced MRI improves detection of brain metastases: a prospective validation of diagnostic yield. J Neurooncol 2016;130(3):485–94.

10. Brant-Zawadzki MN, Gillan GD, Atkinson DJ, Edalatpour N, Jensen M. Three-dimensional MR imaging and display of intracranial disease: improvements with the MP-RAGE sequence and gadolinium. J Magn Reson Imaging 1993;3(4):656–62.

11. Suh CH, Jung SC, Kim KW, Pyo J. The detectability of brain metastases using contrast-enhanced spin-echo or gradient-echo images: a systematic review and meta-analysis. J Neurooncol 2016;129(2):363–71.

12. Hanna SL, Langston JW, Gronemeyer SA. Value of subtraction images in the detection of hemorrhagic brain lesions on contrast-enhanced MR images. AJNR Am J Neuroradiol 1991;12(4):681–5.

13. Ellingson BM, Kim HJ, Woodworth DC, Pope WB, Cloughesy JN, Harris RJ, et al. Recurrent glioblastoma treated with bevacizumab: contrast-enhanced T1-weighted subtraction maps improve tumor delineation and aid prediction of survival in a multicenter clinical trial. Radiology 2013;271(1):200–10.

14. Altman DA, Atkinson DS, Brat DJ. Glioblastoma multiforme. RadioGraphics 2007;27(3):883–8.

15. Mullins ME, Barest GD, Schaefer PW, Hochberg FH, Gonzalez RG, Lev MH. Radiation necrosis versus glioma recurrence: conventional MR imaging clues to diagnosis. Am J Neuroradiol 2005;26(8):1967–72.

16. Scoccianti S, Detti B, Gadda D, Greto D, Furfaro I, Meacci F, et al. Organs at risk in the brain and their dose-constraints in adults and in children: A radiation oncologist's guide for delineation in everyday practice. Radiother Oncol 2015;114(2):230–8.

17. Lasocki A, Gaillard F. Non-contrast-enhancing tumor: a new frontier in glioblastoma research. Am J Neuroradiol 2019 40(5):758-765

18. Dhermain F. Radiotherapy of high-grade gliomas: current standards and new concepts, innovations in imaging and radiotherapy, and new therapeutic approaches. Chin J Cancer 2014;33(1):16–24.

19. Wernicke AG, Smith AW, Taube S, Mehta MP. Glioblastoma: Radiation treatment margins, how small is large enough? Pract Radiat Oncol 2016;6(5):298–305.

20. Hoefnagels FWA, De Witt Hamer P, Sanz-Arigita E, Idema S, Kuijer JPA, Pouwels PJW, et al. Differentiation of edema and glioma infiltration: proposal of a DTI-based probability map. J Neurooncol 2014;120(1):187–98.

21. Rathore S, Akbari H, Doshi J, Shukla G, Rozycki M, Bilello M, et al. Radiomic signature of infiltration in peritumoral edema predicts subsequent recurrence in glioblastoma: implications for personalized radiotherapy planning. J Med Imaging Bellingham 2018;5(2):021219.

22. Cruz LCH da, Rodriguez I, Domingues RC, Gasparetto EL, Sorensen AG. Pseudoprogression and pseudoresponse: imaging challenges in the assessment of posttreatment glioma. Am J Neuroradiol 2011;32(11):1978–85.

23. Hayashida Y, Hirai T, Morishita S, Kitajima M, Murakami R, Korogi Y, et al. Diffusion-weighted imaging of metastatic brain tumors: comparison with histologic type and tumor cellularity. Am J Neuroradiol 2006;27(7):1419–25.

24. Fan GG, Deng QL, Wu ZH, Guo QY. Usefulness of diffusion/perfusion-weighted MRI in patients with non-enhancing supratentorial brain gliomas: a valuable tool to predict tumour grading? Br J Radiol 2006;79(944):652–8.

25. Toh C-H, Castillo M, Wong AM-C, Wei K-C, Wong H-F, Ng S-H, et al. Primary cerebral lymphoma and glioblastoma multiforme: differences in diffusion characteristics evaluated with diffusion tensor imaging. Am J Neuroradiol 2008;29(3):471–5.

26. Smith JS, Cha S, Mayo MC, McDermott MW, Parsa AT, Chang SM, et al. Serial diffusion-weighted magnetic resonance imaging in cases of glioma: distinguishing tumor recurrence from postresection injury. J Neurosurg 2005;103(3):428–38.

27. Kondziolka D, Bernstein M, Resch L, Tator CH, Fleming JFR, Vanderlinden RG, et al. Significance of hemorrhage into brain tumors: clinicopathological study. J Neurosurg 1987;67(6):852–7.

28. Fink KR, Fink JR. Imaging of brain metastases. Surg Neurol Int 2013;4(Suppl 4):S209–19.

29. Jung BA, Weigel M. Spin echo magnetic resonance imaging. J Magn Reson Imaging 2013;37(4):805–17.

30. Mugler JP, Brookeman JR. Three-dimensional magnetization-prepared rapid gradient-echo imaging (3D MP RAGE). Magn Reson Med 1990;15(1):152–7.

31. Barkhof F, Pouwels PJW, Wattjes MP. The Holy Grail in diagnostic neuroradiology: 3T or 3D? Eur Radiol 2011;21(3):449–56.

32. Cattaneo GM, Reni M, Rizzo G, Castellone P, Ceresoli GL, Cozzarini C, et al. Target delineation in post-operative radiotherapy of brain gliomas: Interobserver variability and impact of image registration of MR(pre-operative) images on treatment planning CT scans. Radiother Oncol 2005;75(2):217–23.

33. Wen PY, Chang SM, Van den Bent MJ, Vogelbaum MA, Macdonald DR, Lee EQ. Response assessment in neuro-oncology clinical trials. J Clin Oncol 2017;35(21):2439–49.

34. Ellingson BM, Wen PY, Cloughesy TF. Modified criteria for radiographic response assessment in glioblastoma clinical trials. Neurother 2017;14(2):307–20.

35. van den Bent MJ, Wefel JS, Schiff D, Taphoorn MJB, Jaeckle K, Junck L, et al. Response assessment in neuro-oncology (a report of the RANO group): assessment of outcome in trials of diffuse low-grade gliomas. Lancet Oncol 2011;12(6):583–93.

36. Wen PY, Cloughesy TF, Ellingson BM, Reardon DA, Fine HA, Abrey L, et al. Report of the Jumpstarting Brain Tumor Drug Development Coalition and FDA clinical trials neuroimaging endpoint workshop (January 30, 2014, Bethesda MD). Neuro-Oncol 2014;16 Suppl 7:vii36-47.

37. Ellingson BM, Bendszus M, Boxerman J, Barboriak D, Erickson BJ, Smits M, et al. Consensus recommendations for a standardized brain tumor imaging protocol in clinical trials. Neuro-Oncol 2015;17(9):1188–98.

38. Lescher S, Schniewindt S, Jurcoane A, Senft C, Hattingen E. Time window for postoperative reactive enhancement after resection of brain tumors: less than 72 hours. Neurosurg Focus 2014;37(6):E3.

39. Okada H, Weller M, Huang R, Finocchiaro G, Gilbert MR, Wick W, et al. Immunotherapy response assessment in neuro-oncology: a report of the RANO working group. Lancet Oncol 2015;16(15):e534–42.

40. Henson JW, Ulmer S, Harris GJ. Brain tumor imaging in clinical trials. AJNR Am J Neuroradiol 2008;29(3):419–24.

41. van den Bent MJ, Smits M, Kros JM, Chang SM. Diffuse infiltrating oligodendroglioma and astrocytoma. J Clin Oncol 2017;35(21):2394–401.

42. Chukwueke UN, Wen PY. Use of the Response Assessment in Neuro-Oncology (RANO) criteria in clinical trials and clinical practice. CNS Oncol. 2019;8(1):CNS28

43. Lin NU, Lee EQ, Aoyama H, Barani I, Barboriak DP, Baumert BG, et al. Response assessment criteria for brain metastases: proposal from the RANO group. Lancet Oncol. 2015;16(6):e270-8

44. Young GS. Advanced MRI of adult brain tumors. Neurol Clin 2007;25(4):947–73.

45. Thust SC, Heiland S, Falini A, Jäger HR, Waldman AD, Sundgren PC, et al. Glioma imaging in Europe: A survey of 220 centres and recommendations for best clinical practice. Eur Radiol 2018;28(8):3306–17.

46. Yahya N, Manan HA. Utilisation of diffusion tensor imaging in intracranial radiotherapy and radiosurgery planning for white matter dose optimization: a systematic review. World Neurosurg 2019;130:e188-e198

47. Jain R, Griffith B, Alotaibi F, Zagzag D, Fine H, Golfinos J, et al. Glioma angiogenesis and perfusion imaging: understanding the relationship between tumor blood volume and leakiness with increasing glioma grade. Am J Neuroradiol 2015;36(11):2030–5.

48. Cha S, Yang L, Johnson G, Lai A, Chen M-H, Tihan T, et al. Comparison of microvascular permeability measurements, K(trans), determined with conventional steady-state T1-weighted and first-pass T2*-weighted MR imaging methods in gliomas and meningiomas. AJNR Am J Neuroradiol 2006;27(2):409–17.

49. Horská A, Barker PB. Imaging of brain tumors: MR spectroscopy and metabolic imaging. Neuroimaging Clin N Am 2010;20(3):293–310.

50. Cho Y-D, Choi G-H, Lee S-P, Kim J-K. 1H-MRS metabolic patterns for distinguishing between meningiomas and other brain tumors. Magn Reson Imaging 2003;21(6):663–72.

51. Moreno-Torres Á, Martínez-Pérez I, Baquero M, Campistol J, Capdevila A, Arús C, et al. Taurine detection by proton magnetic resonance spectroscopy in medulloblastoma: contribution to noninvasive differential diagnosis with cerebellar astrocytoma. Neurosurgery 2004;55(4):824–9.

52. Mauri-Fábrega L, Díaz-Sánchez M, Casado-Chocán JL, Uclés-Sánchez AJ. Pseudotumoral forms of multiple sclerosis: report of 14 cases and review of the literature. Eur Neurol 2014;72(1–2):72–8.

53. Renard D, Castelnovo G, Le Floch A, Guillamo J-S, Thouvenot E. Pseudotumoral brain lesions: MRI review. Acta Neurol Belg 2017;117(1):17–26.

54. Majós C, Aguilera C, Alonso J, Julià-Sapé M, Castañer S, Sánchez JJ, et al. Proton MR spectroscopy improves discrimination between tumor and pseudotumoral lesion in solid brain masses. Am J Neuroradiol 2009;30(3):544–51.

55. Harting I, Hartmann M, Jost G, Sommer C, Ahmadi R, Heiland S, et al. Differentiating primary central nervous system lymphoma from glioma in humans using localised proton magnetic resonance spectroscopy. Neurosci Lett 2003;342(3):163–6.

56. Mansour A, Qandeel M, Abdel-Razeq H, Abu Ali HA. MR imaging features of intracranial primary CNS lymphoma in immune competent patients. Cancer Imaging 2014;14(1):22.

57. Neska-Matuszewska M, Zimny A, Bladowska J, Sąsiadek M. Diffusion and perfusion MR patterns of central nervous system lymphomas. Adv Clin Exp Med 2018;27(8):1099–108.

58. Neska-Matuszewska M, Bladowska J, Sąsiadek M, Zimny A. Differentiation of glioblastoma multiforme, metastases and primary central nervous system lymphomas using multiparametric perfusion and diffusion MR imaging of a tumor core and a peritumoral zone—Searching for a practical approach. PLoS ONE 2018;13(1):e0191341

59. Blasel S, Jurcoane A, Franz K, Morawe G, Pellikan S, Hattingen E. Elevated peritumoural rCBV values as a mean to differentiate metastases from high-grade gliomas. Acta Neurochir (Wien) 2010;152(11):1893–9.

60. Zhang J, Liu H, Tong H, Wang S, Yang Y, Liu G, et al. Clinical applications of contrast-enhanced perfusion MRI techniques in gliomas: recent advances and current challenges. Contrast Media Mol Imaging 2017;2017:7064120

61. Scott JN, Brasher PMA, Sevick RJ, Rewcastle NB, Forsyth PA. How often are nonenhancing supratentorial gliomas malignant? A population study. Neurology 2002;59(6):947–9.

62. Law M, Yang S, Wang H, Babb JS, Johnson G, Cha S, et al. Glioma grading: sensitivity, specificity, and predictive values of perfusion MR imaging and proton MR spectroscopic imaging compared with conventional MR imaging. Am J Neuroradiol 2003;24(10):1989–98.

63. Danchaivijitr N, Waldman AD, Tozer DJ, Benton CE, Brasil Caseiras G, Tofts PS, et al. Low-grade gliomas: do changes in rCBV measurements at longitudinal perfusion-weighted MR imaging predict malignant transformation? Radiology 2008;247(1):170–8.

64. Bulik M, Jancalek R, Vanicek J, Skoch A, Mechl M. Potential of MR spectroscopy for assessment of glioma grading. Clin Neurol Neurosurg 2013;115(2):146–53.

65. Li X, Zhu Y, Kang H, Zhang Y, Liang H, Wang S, et al. Glioma grading by microvascular permeability parameters derived from dynamic contrast-enhanced MRI and intratumoral susceptibility signal on susceptibility weighted imaging. Cancer Imaging 2015;15(1):4.

66. Zikou A, Sioka C, Alexiou GA, Fotopoulos A, Voulgaris S, Argyropoulou MI. Radiation necrosis, pseudoprogression, pseudoresponse, and tumor recurrence: imaging challenges for the evaluation of treated gliomas. Contrast Media Mol Imaging 2018:6828396

67. Kessler AT, Bhatt AA. Brain tumour post-treatment imaging and treatment-related complications. Insights Imaging 2018;9(6):1057–75.

68. Verma N, Cowperthwaite MC, Burnett MG, Markey MK. Differentiating tumor recurrence from treatment necrosis: a review of neuro-oncologic imaging strategies. Neuro-Oncol 2013;15(5):515–34.

69. Rock JP, Hearshen D, Scarpace L, Croteau D, Gutierrez J, Fisher JL, et al. Correlations between magnetic resonance spectroscopy and image-guided histopathology, with special attention to radiation necrosis. Neurosurgery 2002;51(4):912–9; discussion 919-920.

70. Thust SC, Bent MJ van den, Smits M. Pseudoprogression of brain tumors. J Magn Reson Imaging 2018;48(3):571–89.

71. Chernov M, Hayashi M, Izawa M, Ochiai T, Usukura M, Abe K, et al. Differentiation of the radiation-induced necrosis and tumor recurrence after gamma knife radiosurgery for brain metastases: importance of multivoxel proton MRS. Minim Invasive Neurosurg 2005;48(4):228–34.

72. Porz N, Bauer S, Pica A, Schucht P, Beck J, Verma RK, et al. Multi-modal glioblastoma segmentation: man versus machine. PLoS ONE 2014;9(5):e96873

73. Fyllingen EH, Stensjøen AL, Berntsen EM, Solheim O, Reinertsen I. Glioblastoma segmentation: comparison of three different software packages. PLOS ONE 2016;11(10):e0164891.

74. Kamnitsas K, Ferrante E, Parisot S, Ledig C, Nori AV, Criminisi A, et al. DeepMedic for brain tumor segmentation. In: Crimi A, Menze B, Maier O, Reyes M, Handels H (Eds.), Brain lesion: Glioma, multiple sclerosis, stroke and traumatic brain injuries. First international workshop, Brainles 2015, held in conjunction with MICCAI 2015, Munich, Germany, October 5, 2015, revised selected papers. Cham: Springer Nature; 2016. Pp. 138–149.

75. Kickingereder P, Andronesi OC. Radiomics, metabolic, and molecular MRI for brain tumors. Semin Neurol 2018;38(1):32–40.

76. Gillies RJ, Anderson AR, Gatenby RA, Morse DL. The biology underlying molecular imaging in oncology: from genome to anatome and back again. Clin Radiol 2010;65(7):517–21.

77. Zacharaki EI, Wang S, Chawla S, Soo Yoo D, Wolf R, Melhem ER, et al. Classification of brain tumor type and grade using MRI texture and shape in a machine learning scheme. Magn Reson Med 2009;62(6):1609–18.

78. Artzi M, Bressler I, Ben Bashat D. Differentiation between glioblastoma, brain metastasis and subtypes using radiomics analysis. J Magn Reson Imaging 2019;50(2):519–28.

79. Chen C, Ou X, Wang J, Guo W, Ma X. Radiomics-based machine learning in differentiation between glioblastoma and metastatic brain tumors. Front Oncol. 2019;9:806.

80. Qian Z, Li Y, Wang Y, Li L, Li R, Wang K, et al. Differentiation of glioblastoma from solitary brain metastases using radiomic machine-learning classifiers. Cancer Lett. 2019;451:128–35.

81. Vamvakas A, Williams SC, Theodorou K, Kapsalaki E, Fountas K, Kappas C, et al. Imaging biomarker analysis of advanced multiparametric MRI for glioma grading. Phys Med 2019;60:188–98.

82. Tan Y, Zhang S-T, Wei J-W, Dong D, Wang X-C, Yang G-Q, et al. A radiomics nomogram may improve the prediction of IDH genotype for astrocytoma before surgery. Eur Radiol 2019;29(7):3325–37.

83. Martin V, Moyal É, Delannes M, Padovani L, Sunyach M-P, Feuvret L, et al. [Radiotherapy for brain tumors: which margins should we apply?] Cancer Radiother 2013;17(5–6):434–43.

84. Niyazi M, Brada M, Chalmers AJ, Combs SE, Erridge SC, Fiorentino A, et al. ESTRO-ACROP guideline “target delineation of glioblastomas.” Radiother Oncol 2016;118(1):35–42.

85. Hu LS, Baxter LC, Smith KA, Feuerstein BG, Karis JP, Eschbacher JM, et al. Relative cerebral blood volume values to differentiate high-grade glioma recurrence from posttreatment radiation effect: direct correlation between image-guided tissue histopathology and localized dynamic susceptibility-weighted contrast-enhanced perfusion MR imaging measurements. AJNR Am J Neuroradiol 2009;30(3):552–8.

86. Prah MA, Stufflebeam SM, Paulson ES, Kalpathy-Cramer J, Gerstner ER, Batchelor TT, et al. Repeatability of standardized and normalized relative cbv in patients with newly diagnosed glioblastoma. AJNR Am J Neuroradiol 2015;36(9):1654–61.

87. Khalifa J, Tensaouti F, Lotterie J-A, Catalaa I, Chaltiel L, Benouaich-Amiel A, et al. Do perfusion and diffusion MRI predict glioblastoma relapse sites following chemoradiation? J Neurooncol 2016;130(1):181–92.

88. Orlandi M, Botti A, Sghedoni R, Cagni E, Ciammella P, Iotti C, et al. Feasibility of voxel-based dose painting for recurrent glioblastoma guided by ADC values of diffusion-weighted MR imaging. Phys Med 2016;32(12):1651–8.

89. Law M, Yang S, Wang H, Babb JS, Johnson G, Cha S, et al. Glioma grading: sensitivity, specificity, and predictive values of perfusion MR imaging and proton MR spectroscopic imaging compared with conventional MR imaging. AJNR Am J Neuroradiol 2003;24(10):1989–98.

90. Laprie A, Catalaa I, Cassol E, McKnight TR, Berchery D, Marre D, et al. Proton magnetic resonance spectroscopic imaging in newly diagnosed glioblastoma: predictive value for the site of postradiotherapy relapse in a prospective longitudinal study. Int J Radiat Oncol Biol Phys 2008;70(3):773–81.

Figure legends

Figure 1. Morphological exploration of a glioblastoma by MRI. a: T1-weighted sequence without contrast; b: fluid-attenuated inversion recovery (FLAIR) sequence; c: T2-weighted sequence; d: diffusion-weighted sequence; e: T1-weighted sequence after contrast enhancement; f: T2* sequence. (a-c) show a temporo-occipital mass with an infiltration of the corpus callosum (arrowhead in b). The mass appears necrotic with hypercellular components in diffusion (d), peripheral enhancement on post-contrast T1-weighted sequence (e). Heterogeneity with potential haemorrhage or microvascular thrombi is detected on T2* sequence (arrowhead in f).

Figure 2. Brain tumour detection and characterization by MRI: use of subtraction map in postoperative setup to detect potential residual tumour. a: T1-weighted sequence showing resection cavity with slight haemorrhage in high spontaneous T1 signal; b: T1-weighted sequence after contrast enhancement is difficult to interpret given the haemorrhage in high T1 intensity; c: Subtraction map confirming enhancement of the anterior part of the cavity (arrowhead).

Figure 3. Brain tumour detection and characterization by MRI: comparison between tumoral infiltration and vasogenic oedema in fluid-attenuated inversion recovery (FLAIR) sequence. a: left temporal grade II glioma presenting with high intensity tumoral infiltration of the cortex, subcortical white matter, and hippocampus; b: left parietal melanoma metastasis surrounded with peripheral oedema in high FLAIR intensity (arrowhead). Note that the oedema does not involve the surrounding cortex.

Figure 4: Glioblastoma assessment with Response Assessment in Neuro-Oncology (RANO) working group criteria. a-d: several T1-weighted sequence after contrast enhancement scans of a glioblastoma are displayed before surgery (a), after surgery (b), 12 weeks after radiotherapy (c) and 24 weeks after radiotherapy (d); e-h: corresponding fluid-attenuated inversion recovery (FLAIR) sequences, before (e) and after surgery (f), 12 weeks (g) and 24 weeks after radiotherapy (h). The reference MRI used for follow-up is the post-radiotherapy scan, in order to take into account early post-radiotherapy changes. Measurement of the lesion (lines in c) consists in two perpendicular axes per enhancing lesions greater than 1cm. A target lesion is individualized (rightmost occipital lesion, 34x19mm) as well as a non-target lesion (leftmost lesion, long axis less than 10mm). Early control (d) shows a preliminary progression of the target lesion (sum of the diameters product: +250%) and a progression of non-target non-enhancing lesions (unequivocal progression of FLAIR hyperintensities in h).

Supplementary figures

Figure S1. Brain tumour detection and characterization by MRI: example of a pseudo tumoral multiple sclerosis in a 25-years patient. a: fluid-attenuated inversion recovery (FLAIR) sequence showing a high intensity lesion in the left corona radiata; b: T1-weighted sequence after contrast enhancement showing an open peripheral enhancement (arrowhead); c: apparent diffusion coefficient (ADC) map showing a peripheral ADC restriction (arrowhead); d: spectroscopy showing a conserved ratio between choline (left asterisk) and *N*-acetyl-aspartate (right asterisk).

Figure S2. Brain tumour detection and characterization *by MRI*: *e*xample of primary cerebral nervous system lymphoma with advanced imaging sequences. a: T1-weighted sequence after contrast enhancement shows multiple enhanced areas of the deep basal nuclei and corpus callosum splenium (arrowheads); b: DWI imaging shows high intensity areas within the enhanced lesion; c: apparent diffusion coefficient (ADC) map shows restricted ADC foci inside the lesion (arrowhead); d: relative cerebral blood volume map does not show increase of relative cerebral blood volume within the lesion (arrowhead); e: tumour perfusion curve (upper curve) does not show increased relative cerebral blood volume (similar area under the curve) as compared to normal brain (lower curve). The typical aspect of signal return above the baseline is highlighted by arrowheads; f: Spectroscopy within the lesion shows an increase choline peak (left asterisk) and decreased *N*-acetyl-aspartate peak (right asterisk), associated with a high lipid peak (triangle).

Figure S3. Brain tumour detection and characterization by MRI: example of fully automatic segmentation with BraTumIA software. The glioblastoma shown in Figure 1 was segmented in less than 2 min. a,b: the segmentation is overlayed onto T1-weighted sequence after contrast enhancement (a) and T2 (b) images. The enhanced portion is overlayed in yellow, the necrosis in red, the infiltration in pink and the oedema in blue (default software colours).

Fig 1a

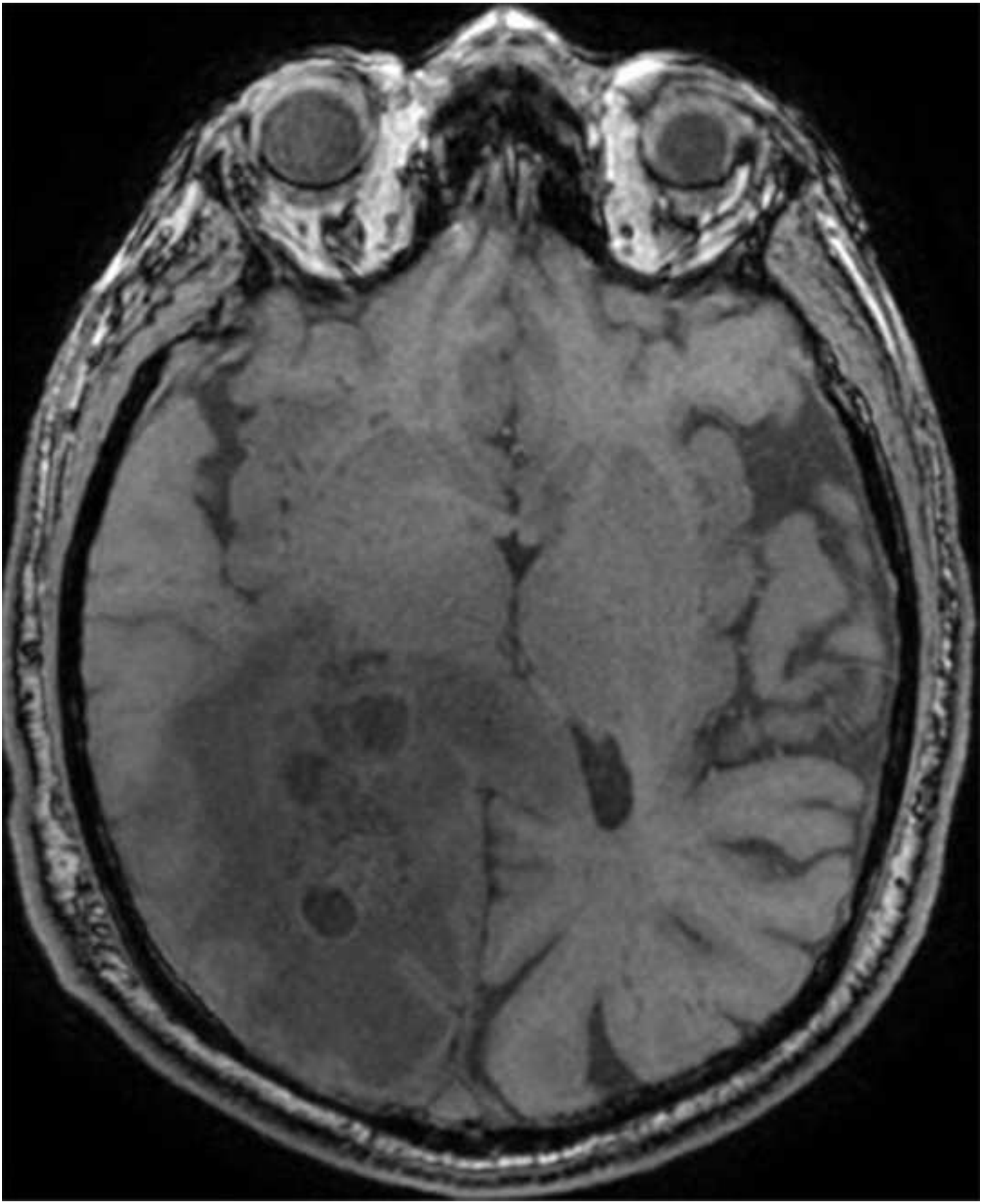

Fig 1b

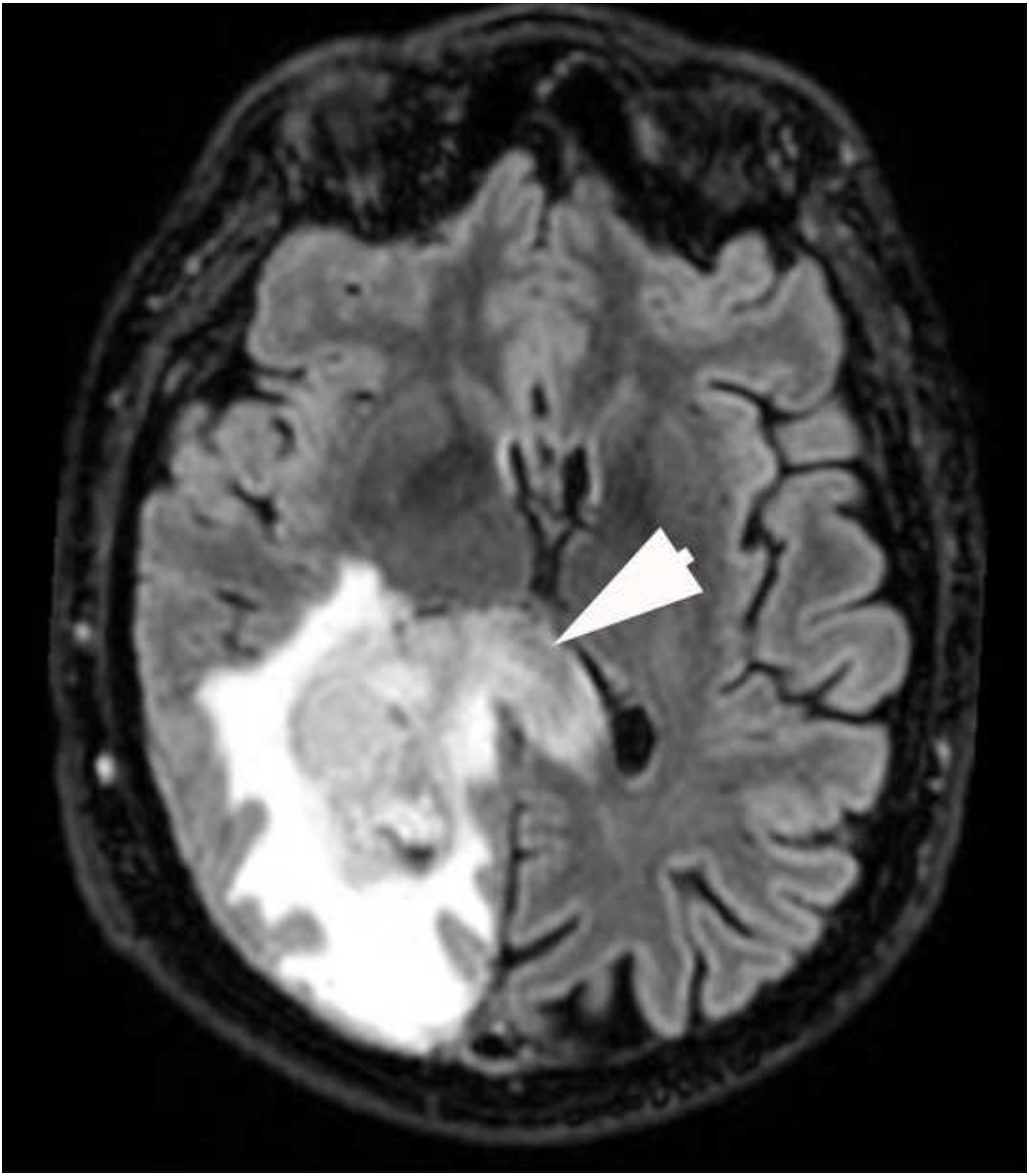

Fig 1c

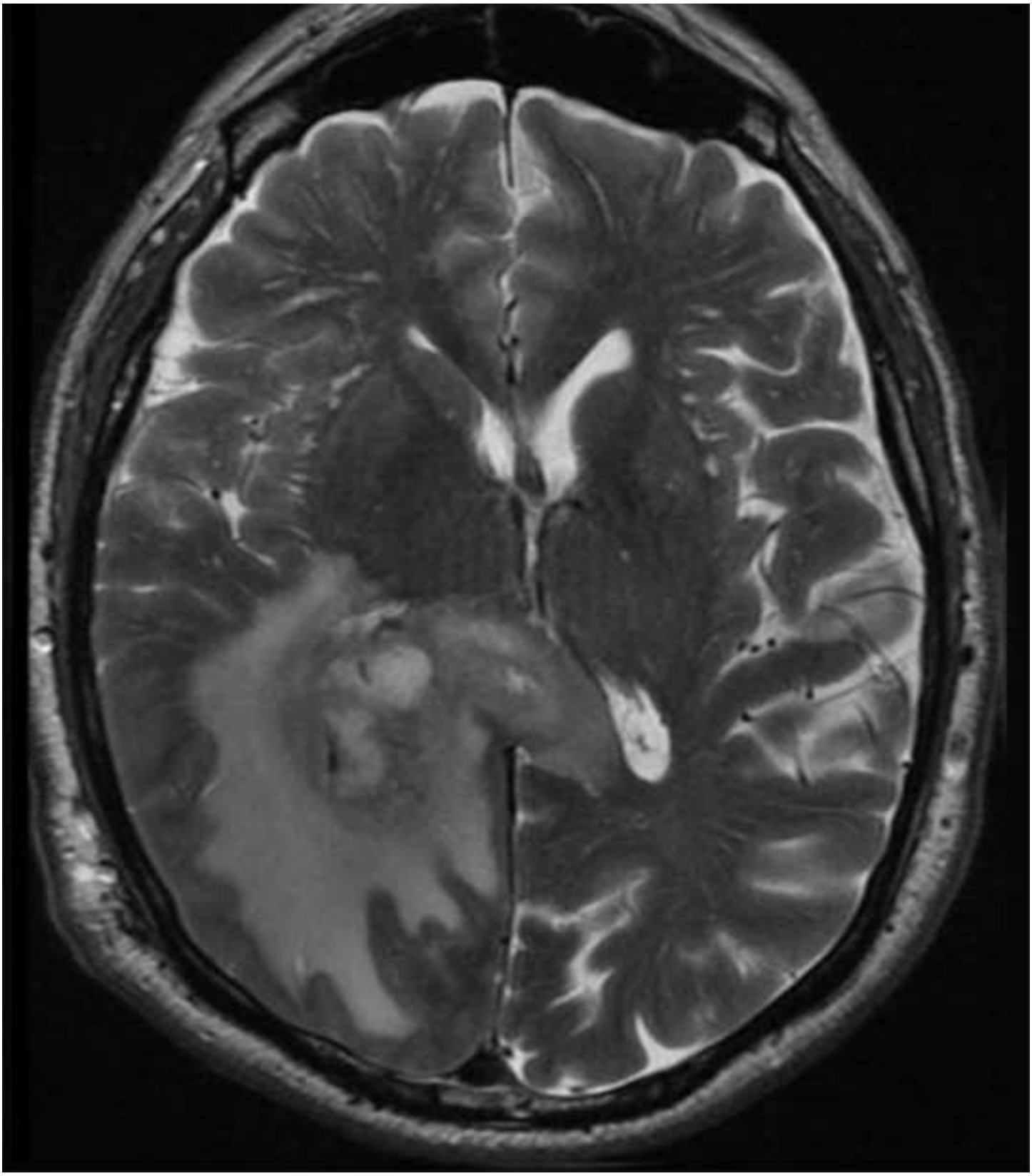

Fig 1d

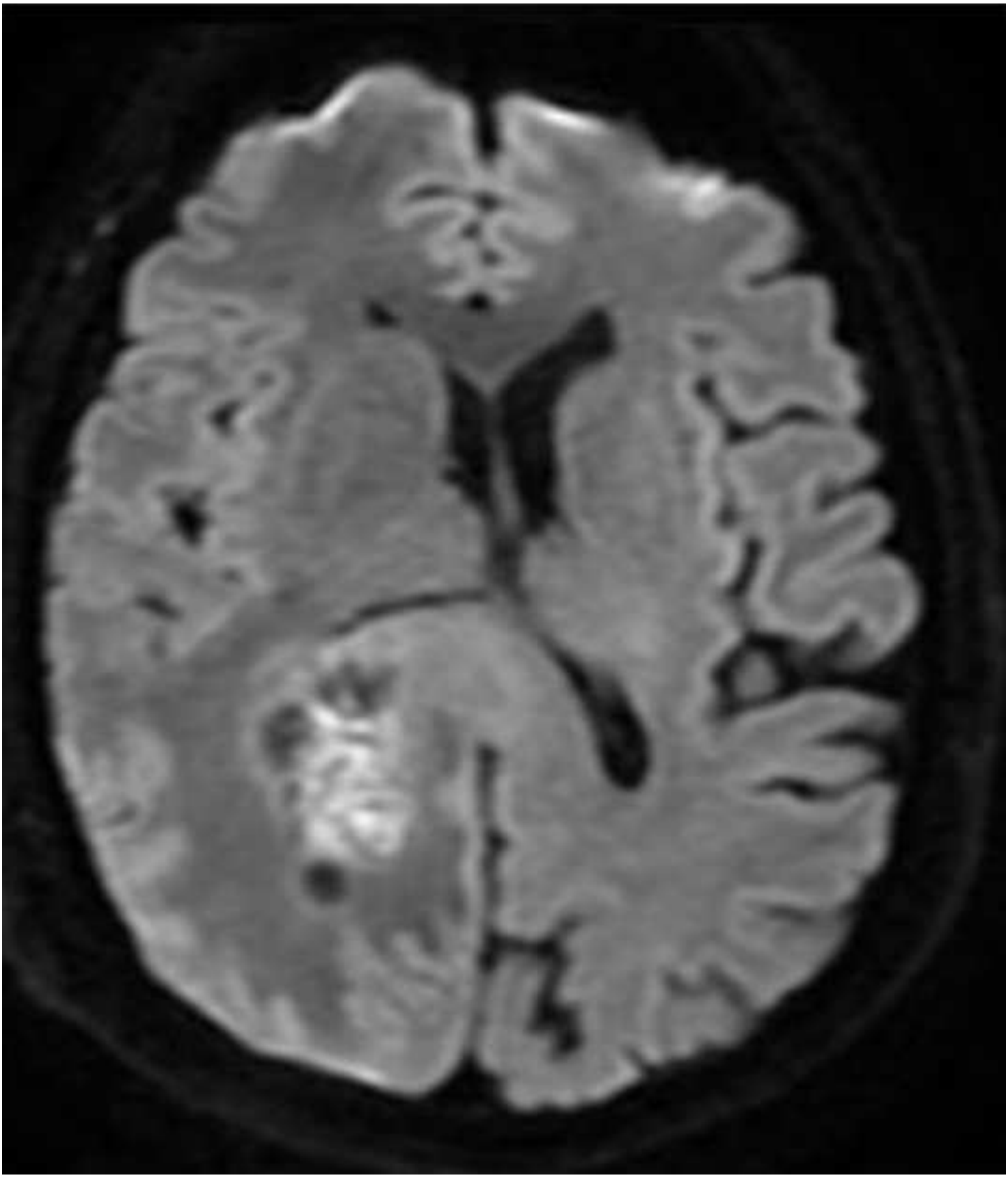

Fig 1e

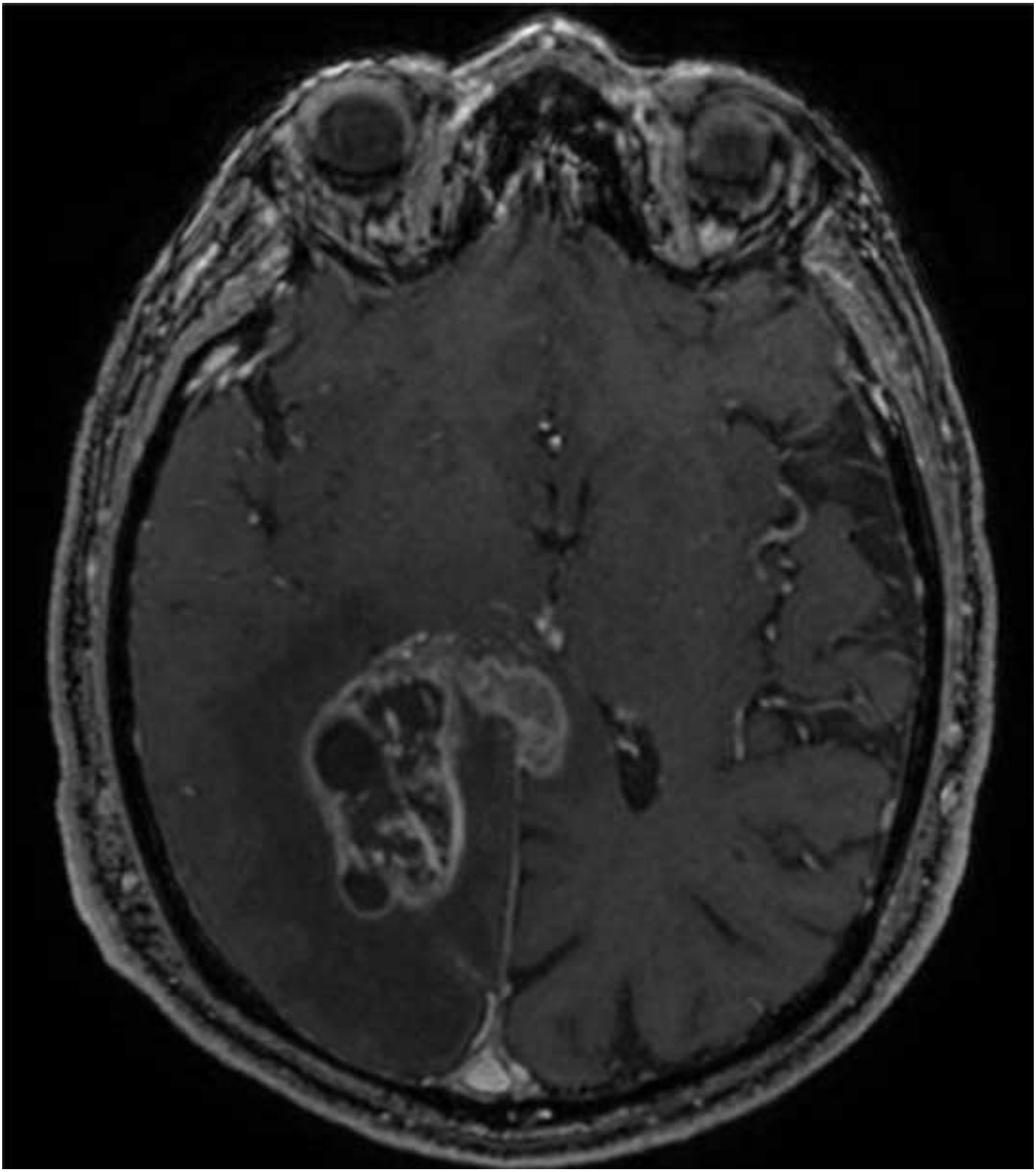

Fig 1f

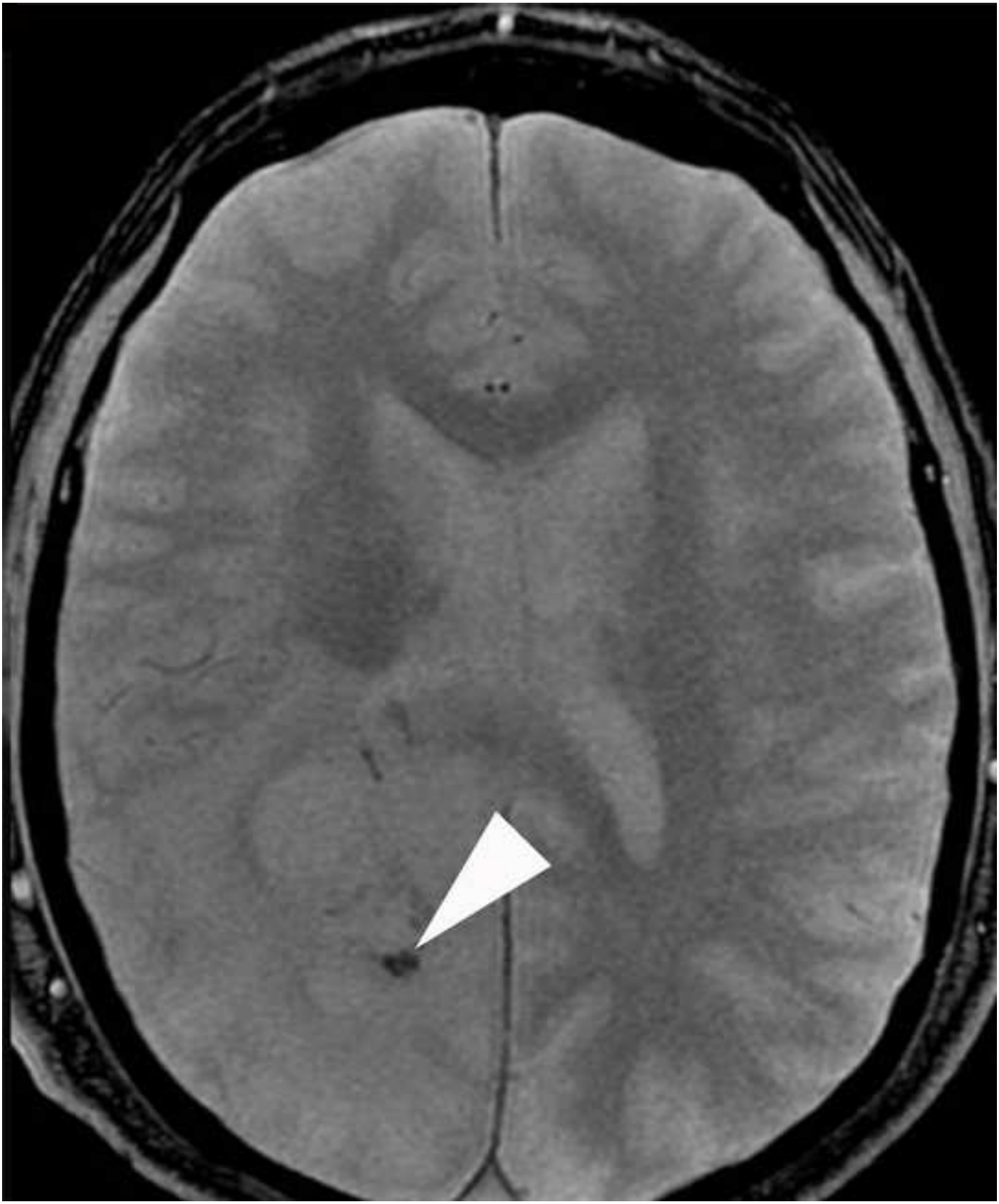

Fig 2a

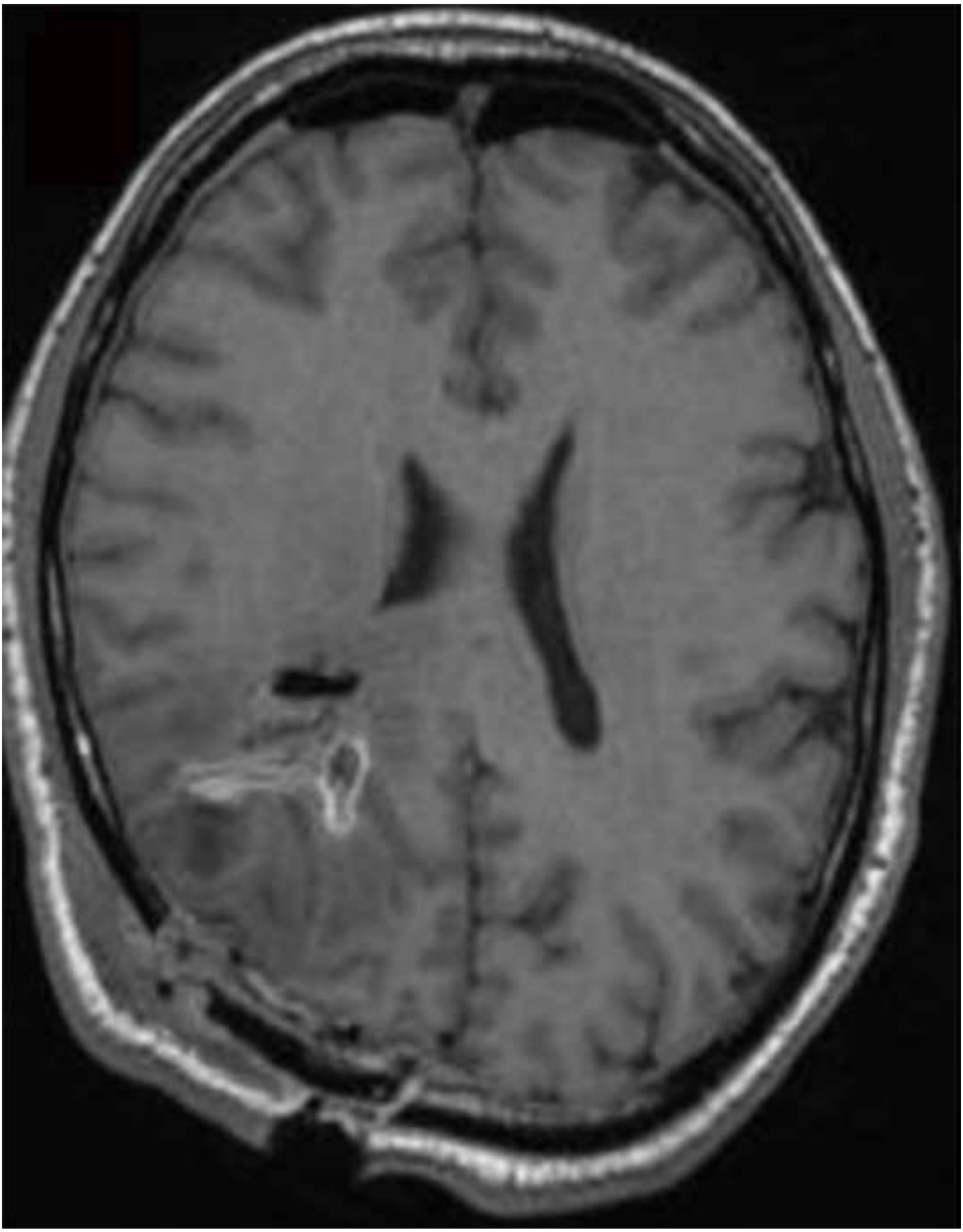

Fig 2b

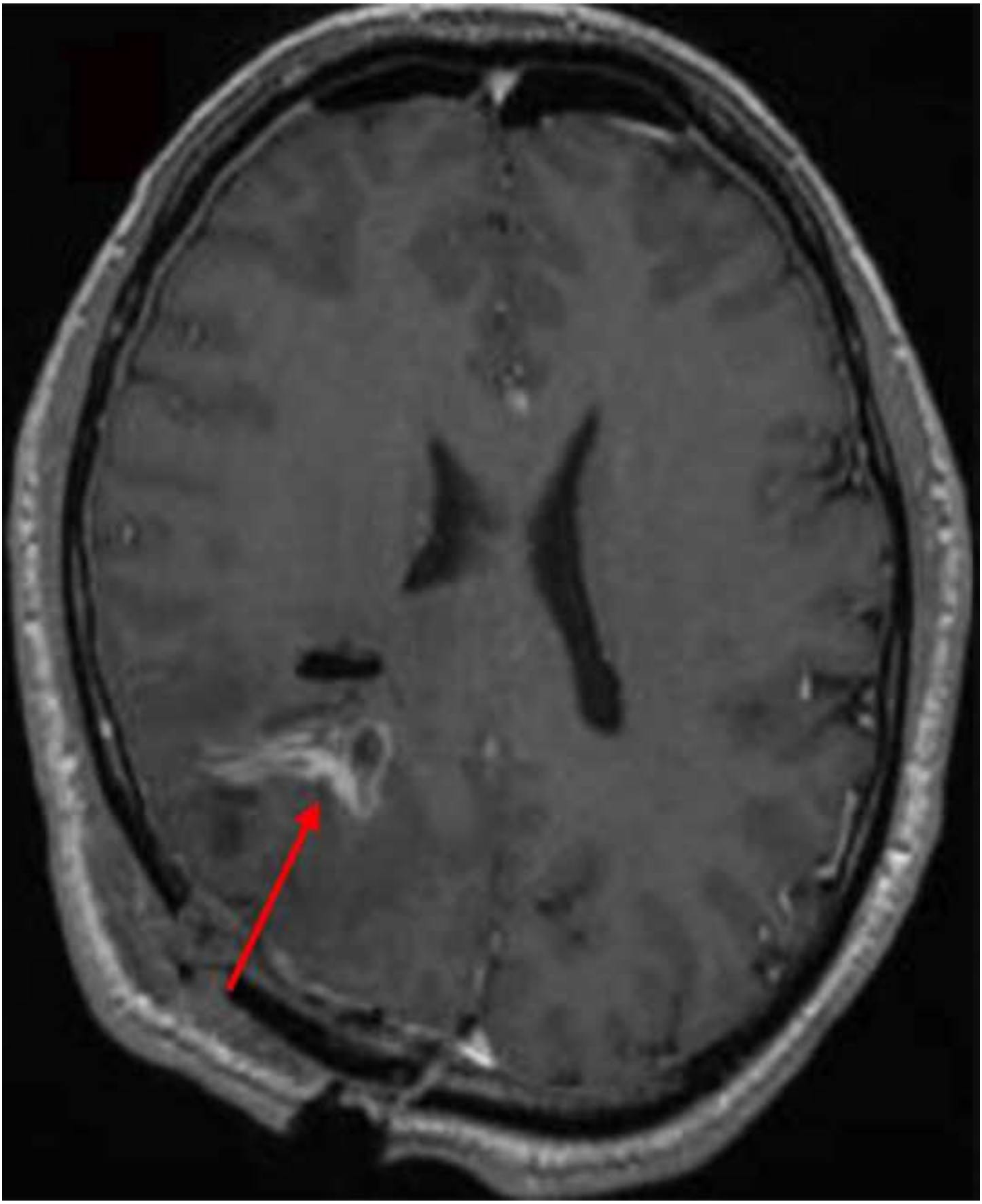

Fig 2c

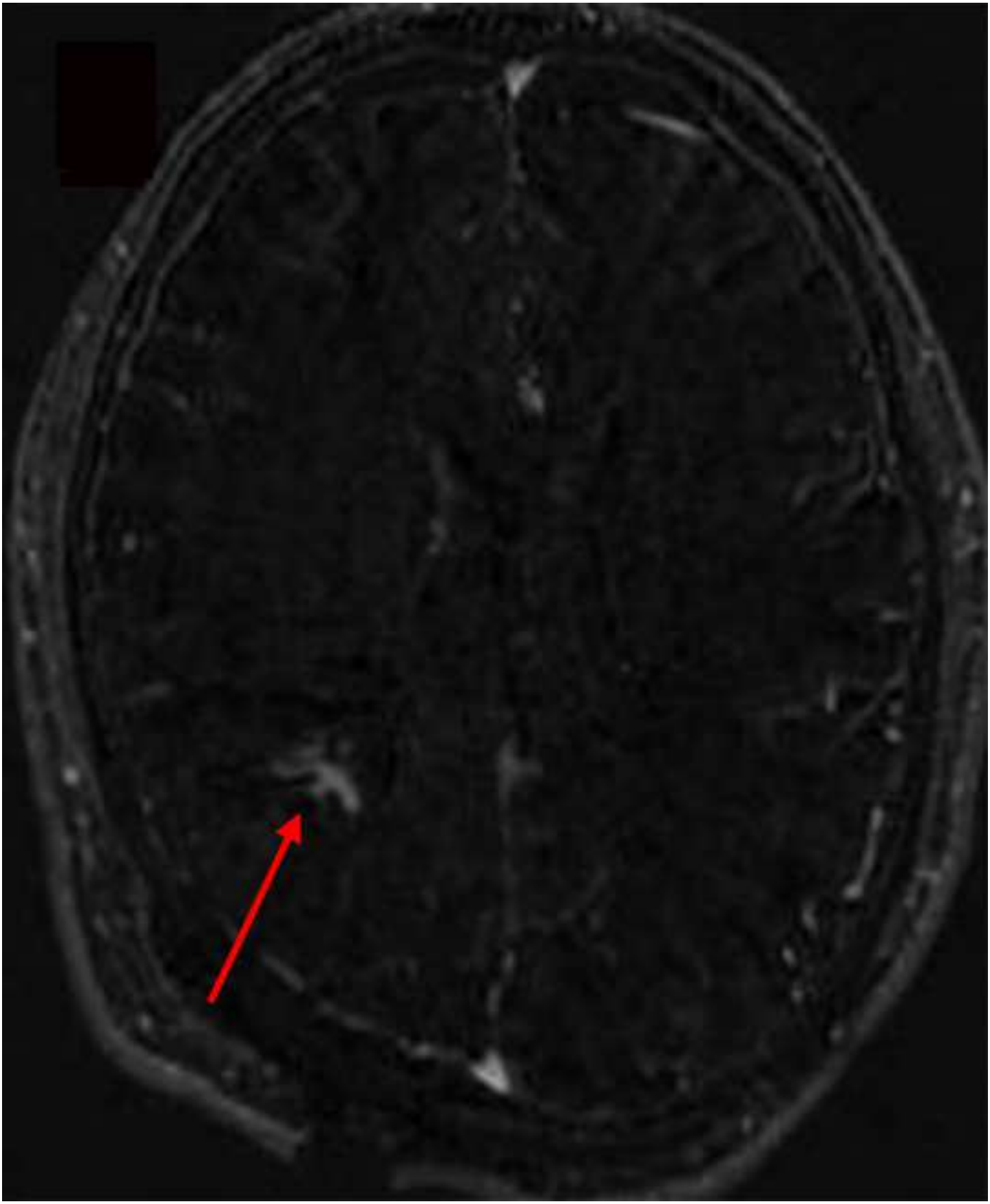

Fig 3a

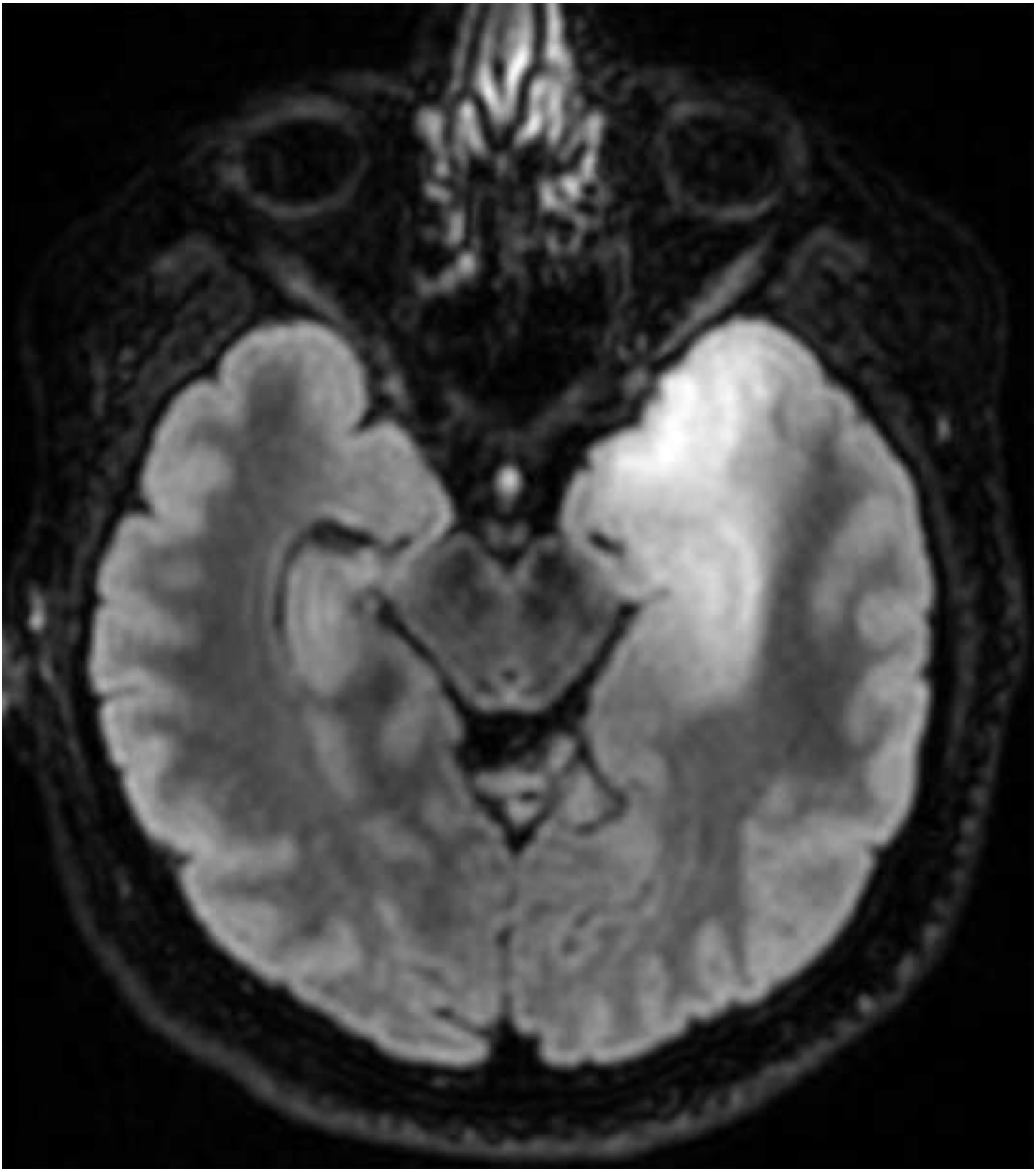

Fig 3b

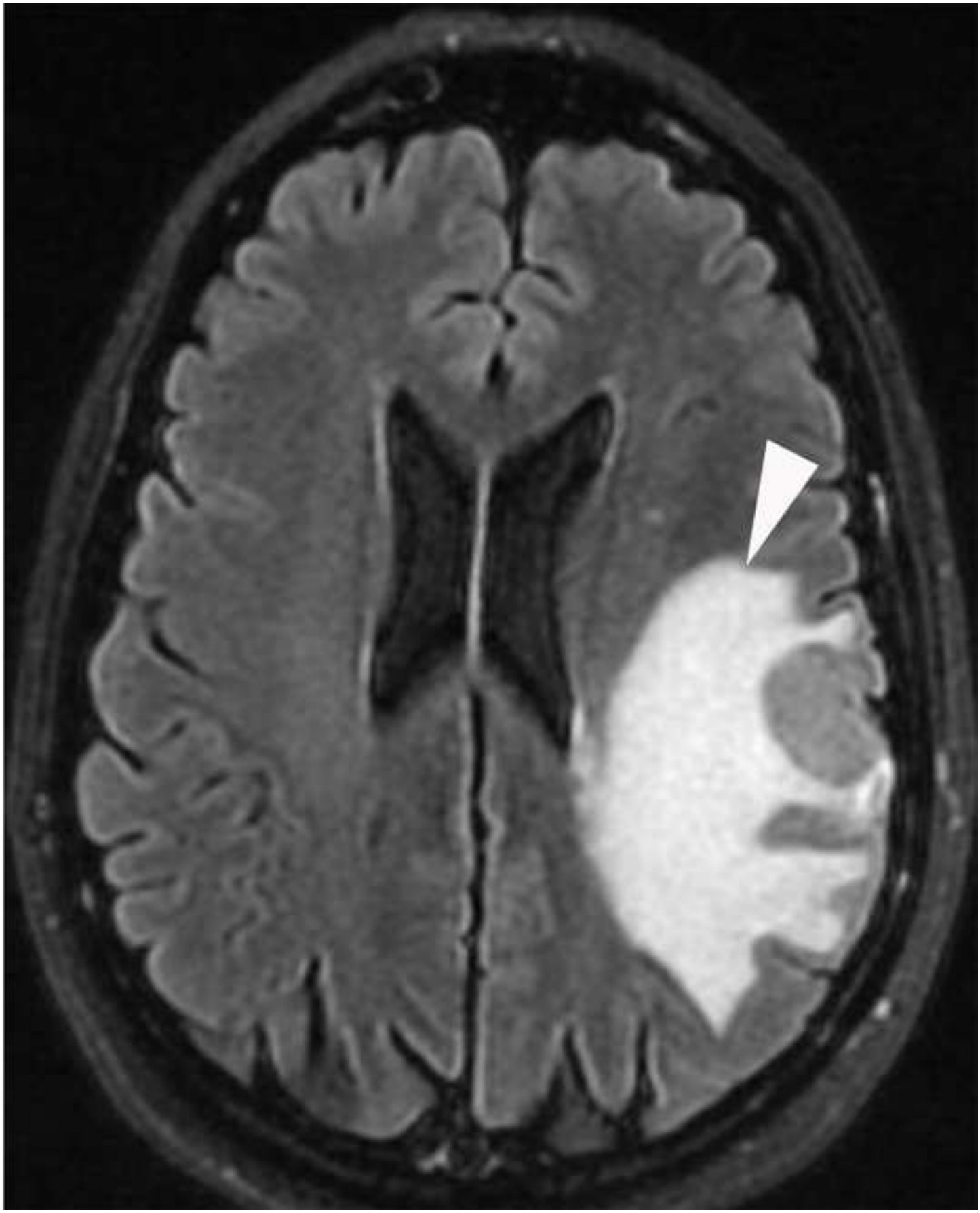

Fig 4a

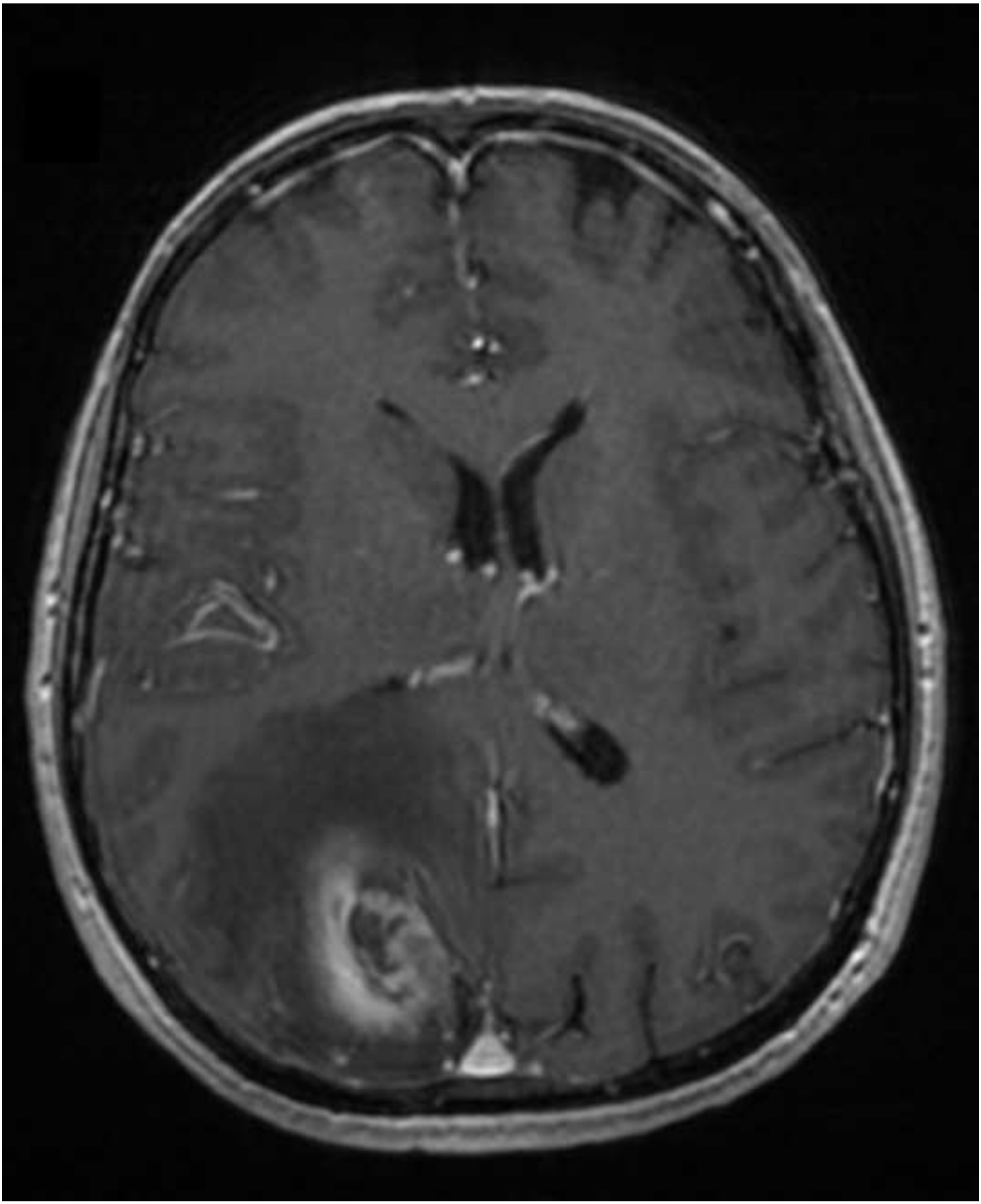

Fig 4b

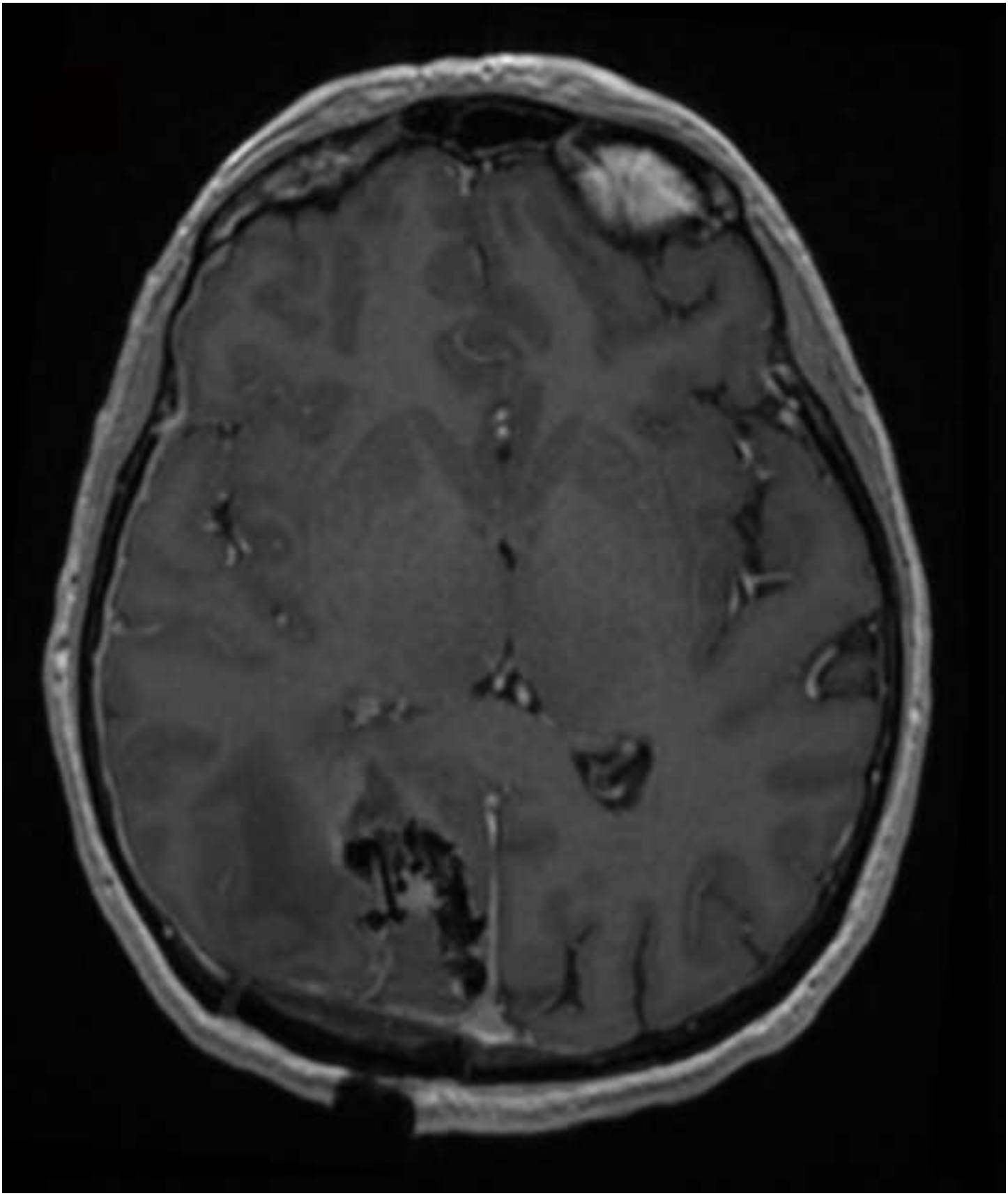

Fig 4c

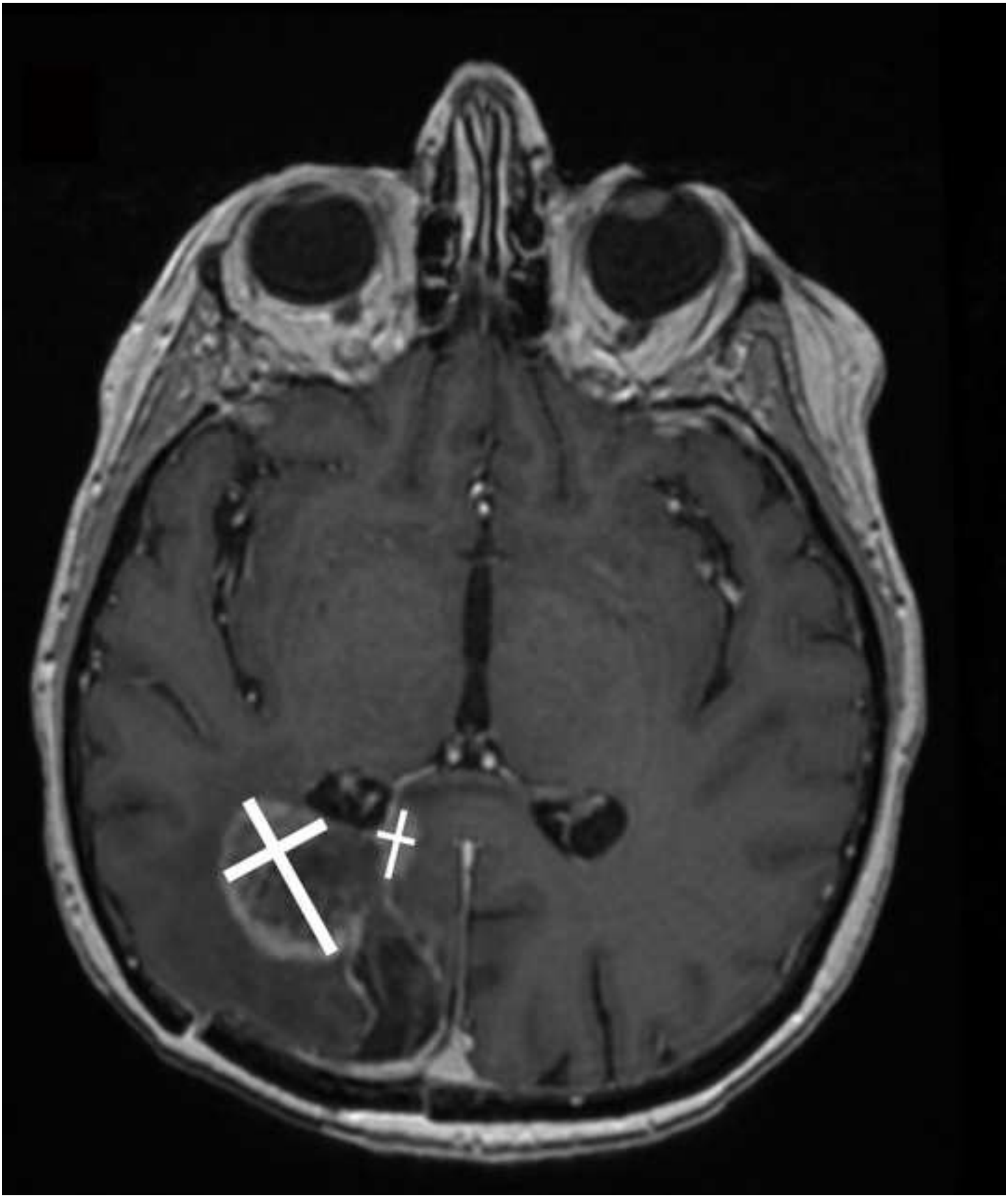

Fig 4d

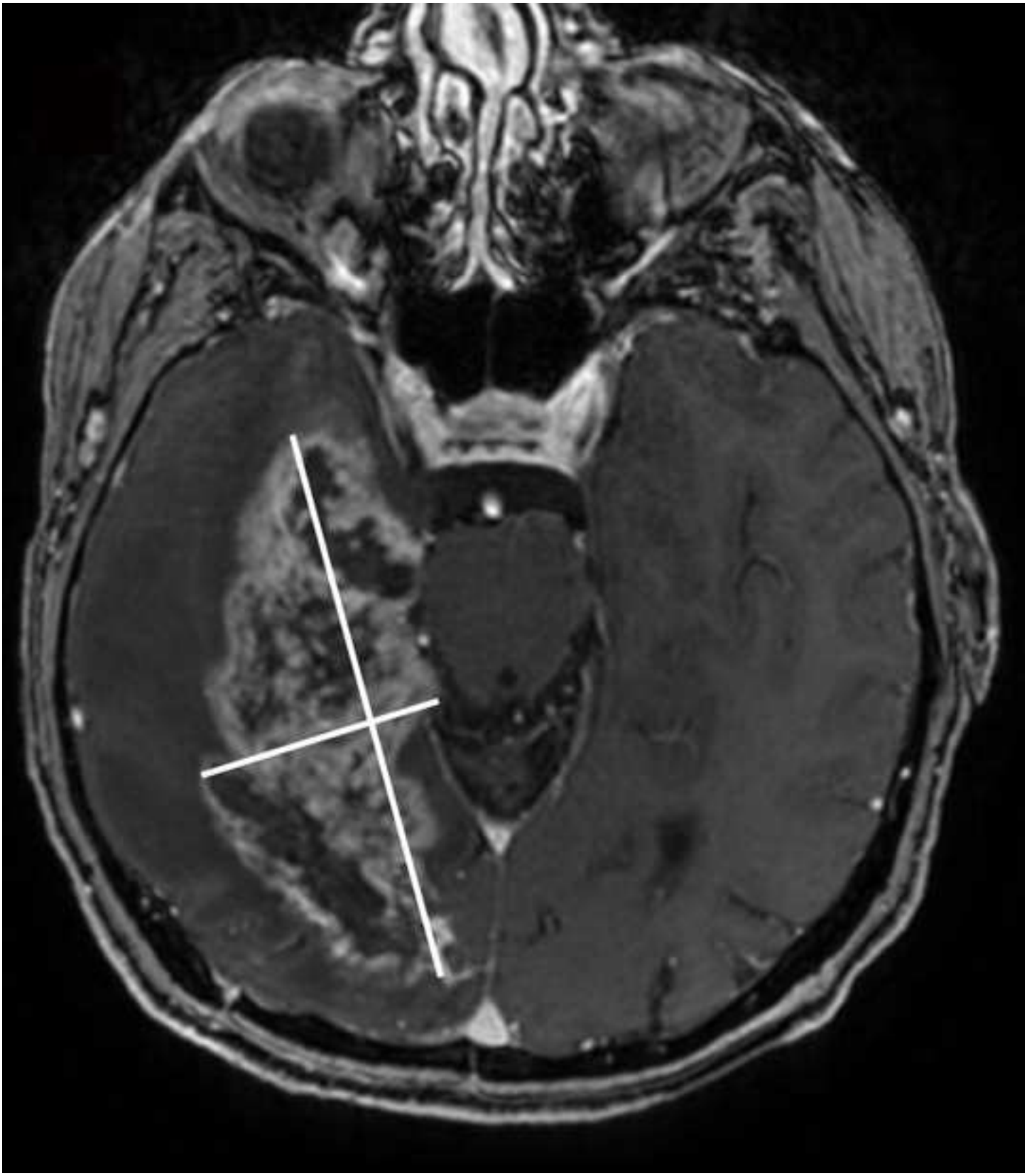

Fig 4e

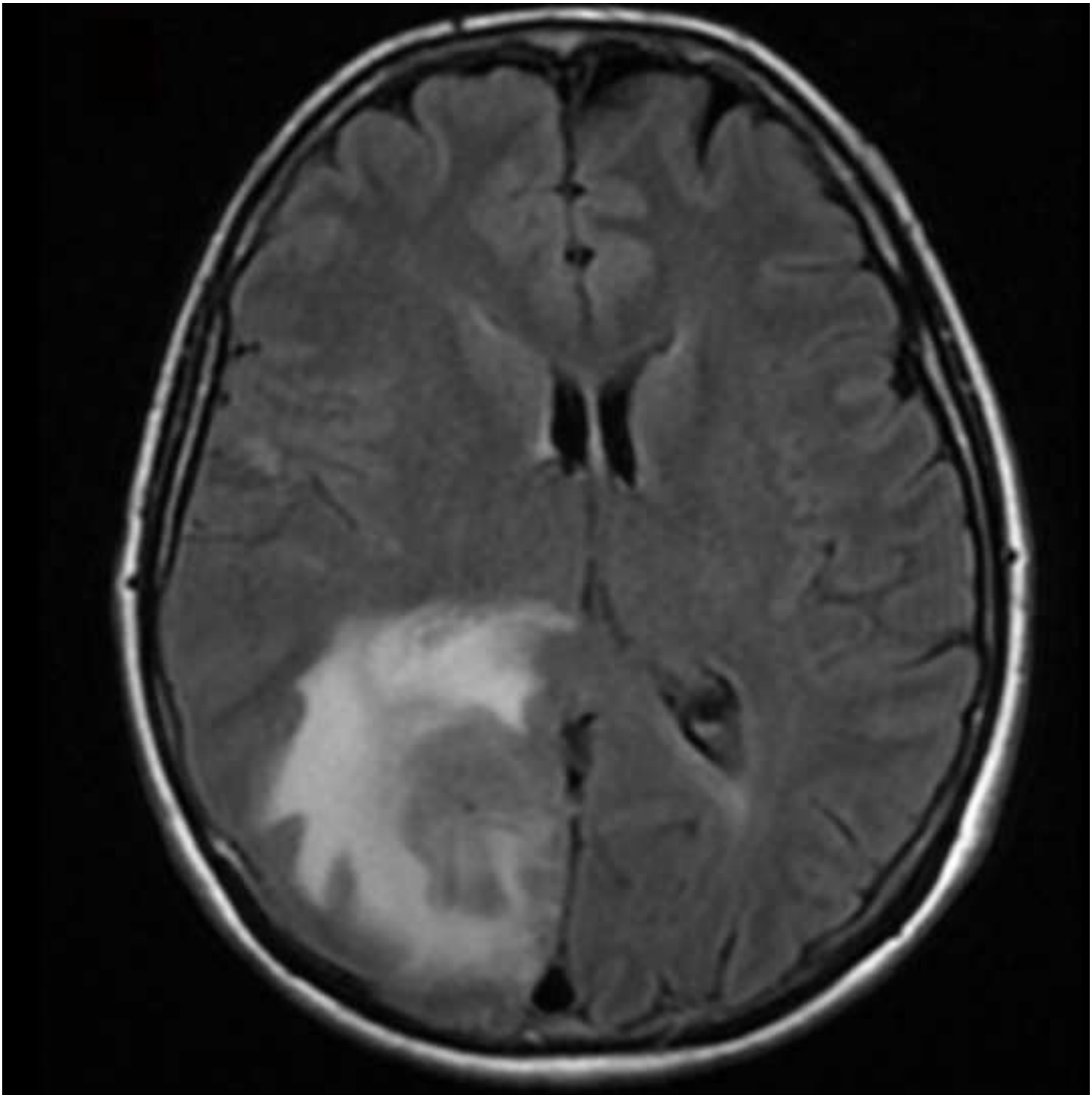

Fig 4f

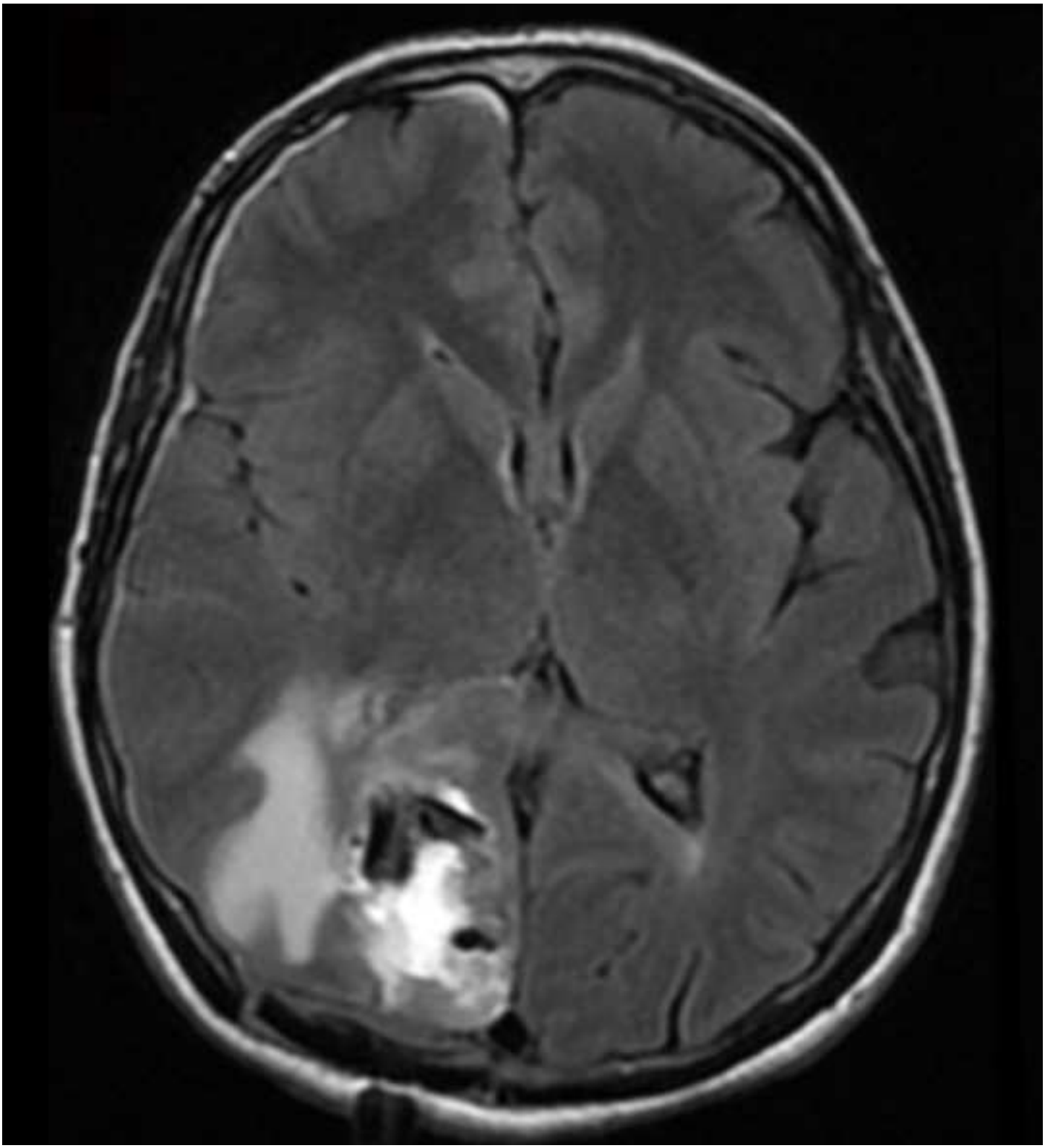

Fig 4g

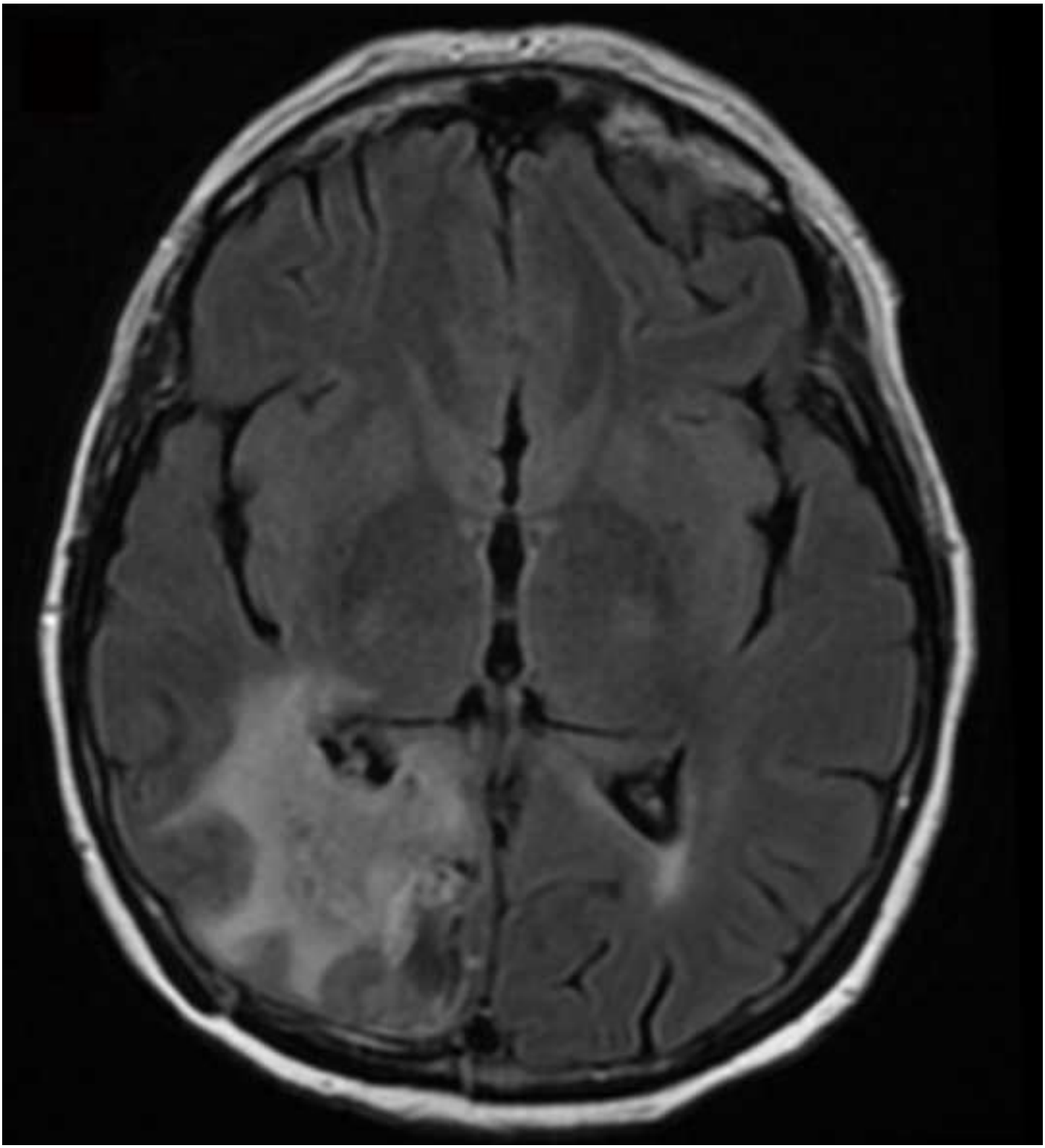

Fig 4h

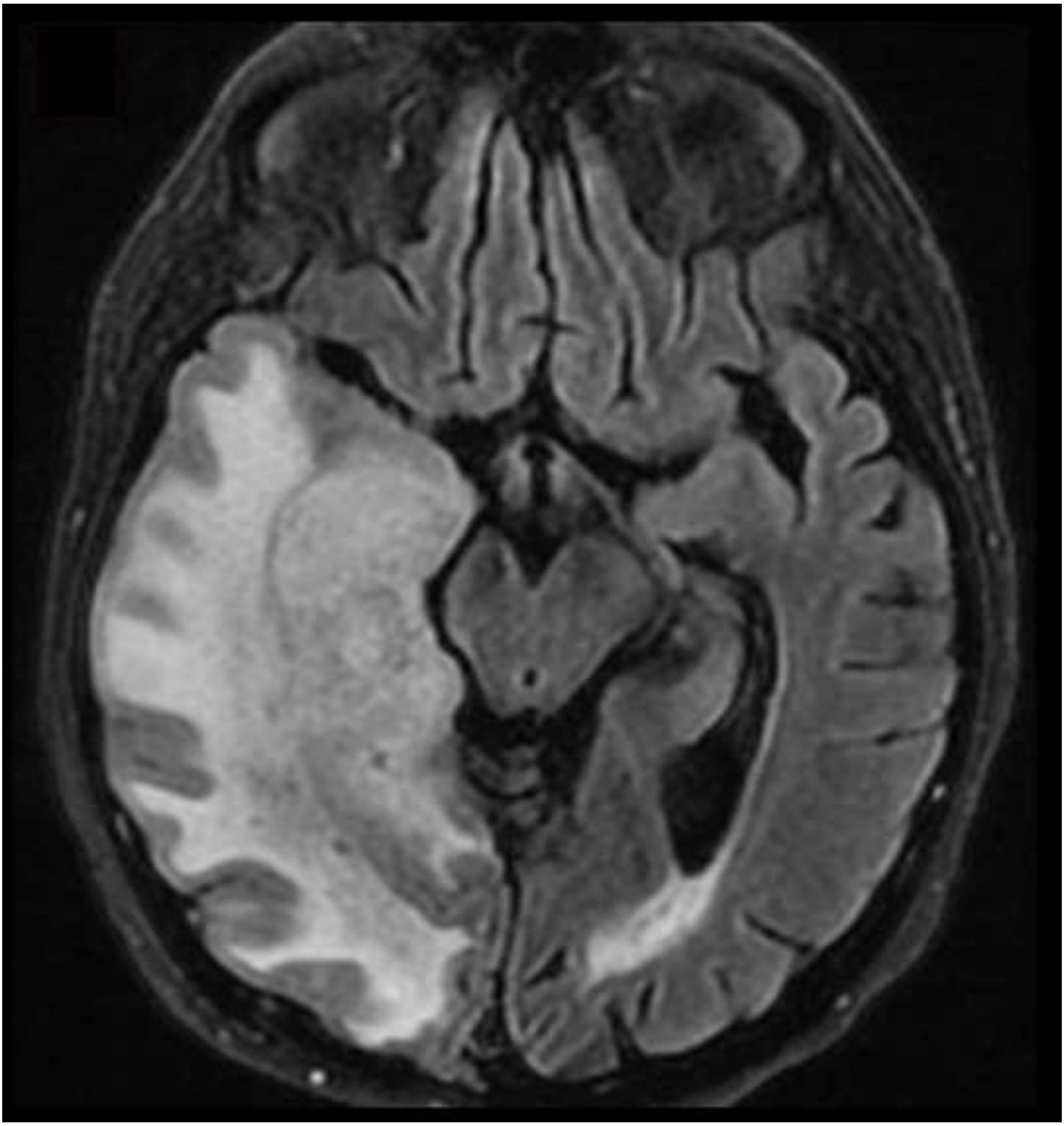

Supplementary Fig S1

Supplementary Fig S2

Supplementary Fig S3

Credit Author Statement

J. Benzakoun : Conceptualization, Investigation, Writing - Original Draft

C. Robert: Conceptualization, Writing - Review & Editing

L. Legrand: Conceptualization, Writing - Review & Editing

J. Pallud: Conceptualization, Writing - Review & Editing

J.F. Meder: Supervision, Writing - Review & Editing

C. Oppenheim: Supervision, Writing - Review & Editing

F. Dhermain : Conceptualization, Investigation, Writing - Original Draft

M. Edjlali : Conceptualization, Investigation, Writing - Original Draft